

A Review on Different Techniques of Mutual Coupling Reduction Between Elements of Any MIMO Antenna. Part 2: Metamaterials and Many More

Original

A Review on Different Techniques of Mutual Coupling Reduction Between Elements of Any MIMO Antenna. Part 2: Metamaterials and Many More / Kumar, A., Ansari, A.Q., Kanaujia, B.K., Kishor, J., Matekovits, L.. - In: RADIO SCIENCE. - ISSN 0048-6604. - ELETTRONICO. - 56:3(2021). [10.1029/2020RS007222]

Availability:

This version is available at: 11583/2877545 since: 2021-03-27T18:17:07Z

Publisher:

American Geophysical Union

Published

DOI:10.1029/2020RS007222

Terms of use:

This article is made available under terms and conditions as specified in the corresponding bibliographic description in the repository

Publisher copyright

(Article begins on next page)

Radio Science

REVIEW ARTICLE

10.1029/2020RS007222

Key Points:

- Mutual coupling (MC) reduction among antenna elements is a significant challenge while designing a compact MIMO antenna design
- The negative permittivity and permeability property of Metamaterials helps in suppressing the ground wave propagation
- Some more MC reduction techniques have been discussed thoroughly in this article, like Electromagnetic Band Gap (EBG) structure, Decoupling and Matching network, and Neutralization line

Correspondence to:

L. Matekovits,
ladislau.matekovits@polito.it

Citation:

Kumar, A., Ansari, A. Q., Kanaujia, B. K., Kishor, J., & Matekovits, L. (2021). A review on different techniques of mutual coupling reduction between elements of any MIMO antenna. Part 2: Metamaterials and many more. *Radio Science*, 56, e2020RS007222. <https://doi.org/10.1029/2020RS007222>

Received 15 OCT 2020

Accepted 24 JAN 2021

© 2021. American Geophysical Union.
All Rights Reserved.

A Review on Different Techniques of Mutual Coupling Reduction Between Elements of Any MIMO Antenna. Part 2: Metamaterials and Many More

Amit Kumar¹ , Abdul Quaiyum Ansari² , Binod Kumar Kanaujia³ , Jugul Kishor⁴ , and Ladislau Matekovits^{5,6,7} 

¹Department of Electrical and Electronics Engineering, Darbhanga College of Engineering, Darbhanga, India,

²Department of Electrical Engineering, FET, Jamia Millia Islamia, New Delhi, India, ³School of Computational and Integrative Sciences, Jawaharlal Nehru University, New Delhi, India, ⁴Department of Electronics and Communication Engineering, JIMS Engineering Management Technical Campus, Greater Noida, India, ⁵Dipartimento di Elettronica e Telecomunicazioni, Politecnico di Torino, Torino, Italy, ⁶Faculty of Electronics and Telecommunications, Politehnica University Timisoara, Timisoara, Romania, ⁷Istituto di Elettronica e di Ingegneria dell'Informazione e delle Telecomunicazioni, National Research Council, Turin, Italy

Abstract This two-part article presents a review of different techniques of mutual coupling (MC) reduction. MC reduction is a primary concern while designing a compact multiple-input-multiple-output (MIMO) antenna where the separation between the antennas is less than $\lambda_0/2$, that is, half of the free-space wavelength. The negative permittivity and permeability of artificially created materials/structures (Metamaterials) significantly help reduce MC among narrow-band compact MIMO antenna design elements. In this part two of the review paper, we will discuss techniques: Metamaterials; Split-Ring-Resonator; Complementary-Split-Ring-Resonator; Frequency Selective Surface, Metasurface, Electromagnetic Band Gap structure, Decoupling and Matching network, Neutralization line, Cloaking Structures, Shorting vias and pins and few more.

1. Introduction

The demand for high-data rate wireless transmission in compact handheld devices like smartphones has revolutionized the importance of compact multiple-input-multiple-output (MIMO) antenna design, which can fulfill the increasing demand without sacrificing the additional bandwidth or increased transmit power (A. Kumar, Ansari, Kanaujia, & Kishor, 2018; A. Kumar, Ansari, Kanaujia, Kishor, & Tewari, 2018) in a rich scattering environment. Along with high-data rates, spatial diversity, and pattern diversity among antenna elements are also required to minimize the power losses and maximize the performance (A. Kumar et al., 2019).

The MIMO antenna should have a common ground embedded on a single substrate and share at least one common resonating frequency. It will ease the integration in monolithic integrated circuits (A. Kumar et al., 2020). We will find many MIMO antennas having no common ground, but such cases should be avoided because of various reasons, as stated by Sharawi (2017).

Compact MIMO antenna results in strong MC among antenna elements that needs to be reduced. Usually, negative permittivity and permeability are not found in naturally occurring materials. Still, they can be produced by some artificial structures like split-ring-resonators (SRRs) (Pendry et al., 1999), which helps in curbing the MC effects. Some periodic structures like electromagnetic band gap (EBG) structures (Kapoor, 2013) are also significant in reducing MC.

This article deals with a thorough description of the existing isolation techniques apart from defected ground structures (DGSs) and Parasitic Structures, which are already discussed in part one of this article for minimizing the MC between patch antennas present until the to date literature. We will also observe and discuss various MC reduction techniques' performance through the comparison tables, highlighting its importance as per the different types of operation bands like narrow-band, wideband, or ultrawideband.

Many review papers (Chouhan et al., 2018; Irene & Rajesh, 2018b; Malviya et al., 2017; Nadeem & Choi, 2019) have been published, citing various techniques of MC reduction but were limited to some specific design and parameters. The main objective is to have closely spaced MIMO antenna elements with high isolation between them. The techniques which we are to discuss in part two of the two-part article are tabulated in Table 1. We will discuss these techniques one by one in detail in the next section.

Besides the techniques, mentioned in Table 1, we can observe that *Frequency Selective Surface (FSS)* (Huang, 2020) and *Metasurface* (F. Liu et al., 2020; Z. Wang et al., 2020; Yin et al., 2020) are also sometimes useful in suppressing MC along with their many others advantages.

2. Isolation Techniques Discussion

2.1. Metamaterials

Materials which do not exist in nature, but can be artificially designed to have the property of single negative (either ϵ_r or μ_r is negative) or double negative (DNG) (both ϵ_r and μ_r are negative) are termed as “Metamaterials (MTMs)”. When both the properties are negative, the material is termed as DNG MTM and will act as a black hole where electromagnetic waves cannot propagate. In 1968, V. G. Veselago (1968) was the first one to find the phenomenon of effective negative permeability and permittivity in the artificially created structures, which has changed the outlook for the existing materials in nature. Before that, materials were supposed to always exhibit positive permeability and permittivity. The research has got another dimension when (Pendry et al., 1999) have discovered that the SRR structure will show an effective negative magnetic permeability effect when kept in the proximity of an existing electromagnetic field. These artificial materials may have negative permittivity or permeability, or both. The effective permittivity and permeability of metamaterials can be calculated from its reflection and transmission coefficients. The proposed method has been comprehensively explained by D. R. Smith and S. Schultz (Smith et al., 2002) in 2002.

Similarly, effective permittivity and permeability for a novel V-shaped MTMs have been investigated (Ekmeççi & Turhan-Sayan, 2007) through simulated S-parameters. The Magnetic response of SRR at microwave frequencies and its properties and equivalent circuit diagram has been thoroughly discussed in K. Aydin & Ozbay (2006), Baena et al. (2005), Katsarakis et al. (2004), Koray. Aydin et al. (2005) and Sauviac et al. (2004). The magnetic resonance of the MTM-SRR can be controlled as described in J. Wang et al. (2008), where the inner ring of the SRR has been rotated while in K. Aydin and Ozbay (2007) SRRs loaded with capacitor have been used to shift the magnetic resonance frequency as per the requirements. MTMs have artificial magnetism but can also exhibit negative refractive index—a property not found in any known naturally occurring material; (Padilla et al., 2006; Smith et al., 2004) have shown the remarkable potential of MTMs to explore new horizons in electromagnetism. A review paper has discussed various MTMs based isolation structures in the MIMO antenna field (Gangwar et al., 2014). MTMs are broadly classified into SRR, CSRR, and FSS. We have emphasized on the discussion and observation of some of the novel and famous structures to overview the existing MTMs useful for MC reduction. A square SRR has been placed at the back of the planar antenna (J. Y. Lee et al., 2015) to suppress the MC, as represented in Figure 1a. The SRR has been acting as a wave trap. A pair of SRR has been placed between the rectangular patch antenna (M. U. Khan & Sharawi, 2014; A. Kumar, Ansari, Kanaujia, & Kishor, 2018), while three CSRRs are loaded on its ground plane (Ramachandran et al., 2016), and four SRRs are arranged together to form a ring (Ramachandran et al., 2017) to suppress the MC as represented in Figures 1b–1d respectively. Among many of the popular methods based on MTMs, some are mentioned here: CSRR loaded ground (S. Kumar et al., 2018), three pairs of slotted-CSRRs (Bait-Suwailam, Siddiqui, et al., 2010) as represented in Figure 2a, single-negative magnetic (MNG) MTM (Bait-Suwailam, Boybay, et al., 2010) as described in Figure 2b, square-shaped CSRR (Selvaraju et al., 2018a), Hilbert-shaped magnetic waveguided MTMs (H. X. Xu et al., 2013), three-dimensional (3-D) novel MTM structures (K. Yu et al., 2018), bridge square SRR (Al-fayyadh & Alsabbagh, 2017), MTM-inspired resonators (Hsu et al., 2011; Iqbal et al., 2018), SRR along with DGS (Irene & Rajesh, 2018a), capacitively loaded loop MTM superstrate (Alibakhshikenari, Salvucci, et al., 2018; Jafarholi et al., 2019), epsilon-near-zero metamaterials (Mazaheri & Jafarholi, 2018), two columns of opposite faced CSRR (Selvaraju et al., 2018b),

Table 1
Mutual Coupling Reduction Techniques With References

Techniques	References
Metamaterials (MTMs)-Split-Ring-Resonator (SRR); Complementary-Split-Ring-Resonator (CSRR)	(Al-fayyadh & Alsabbagh, 2017; Alibakhshikenari, Salvucci, et al., 2018; Aydin & Ozbay, 2006, 2007; Koray. Aydin et al., 2005; Baena et al., 2005; Bait-Suwailam, Boybay, et al., 2010; Bait-Suwailam, Siddiqui, et al., 2010; Bilal et al., 2017; Dadgarpour et al., 2017; Ekmekçi & Turhan-Sayan, 2007; Gangwar et al., 2014; Garg & Jain, 2020; Guo et al., 2019; Hsu et al., 2011; Iqbal et al., 2018; Irene & Rajesh, 2018a; Jafargholi et al., 2019; Katsarakis et al., 2004; M. U. Khan & Sharawi, 2014; Krishna et al., 2016; A. Kumar, Ansari, Kanaujia, & Kishor, 2018; A. Kumar, Ansari, Kanaujia, Kishor, & Kandpal, 2018; J. Y. Lee et al., 2015; M. Li et al., 2020; Mark et al., 2020; Mazaheri & Jafargholi, 2018; Najafy & Bemani, 2020; Ntaikos & Yioultsis, 2013; Öznazi & Ertürk, 2008; Padilla et al., 2006; Pendry et al., 1999; Qamar et al., 2016, 2014; Ramachandran et al., 2017, 2016; Sauviac et al., 2004; Selvaraju et al., 2018b, 2018a; Shafique et al., 2015; Smith et al., 2004; 2002; M. C. Tang et al., 2017; Thummaluru & Chaudhary, 2017; Torabi et al., 2016; Veselago, 1968; F. Wang et al., 2018; J. Wang et al., 2008; G. C. Wu et al., 2015; Xu et al., 2013; K. Yu et al., 2018; Zhai et al., 2015; X. Zhu et al., 2017; Ziolkowski & Engheta, 2020)
Electromagnetic Band Gap (EBG)	(Abdelgwad & Ali, 2020; Abedin & Ali, 2005; Abidin et al., 2018; Al-Fayyadh et al., 2017; Alam et al., 2013; Alibakhshikenari, Virdee, et al., 2018; Alibakhshikenari et al., 2019a, 2019b; Chen et al., 2018; Dabas et al., 2018; Ebadi & Semnani, 2014; Exposito-Dominguez et al., 2012; Farahani et al., 2010; Iqbal et al., 2019; Islam & Alam, 2013; J. D. Shumpert, T. J. Ellis, G. M. Rebeiz, 1997; T. T. Jiang et al., 2018; John, 1987; Kapoor, 2013; Kim et al., 2011; J. Kumar, 2016; N. Kumar & Kommuri, 2019; Y. Lee & Sun, 2008; Q. Li et al., 2014; Lu & Lin, 2013; Manimegalai, 2014; Mavridou et al., 2016; Mohamadzade & Afsahi, 2017; Mohamed et al., 2019; Mu'ath J et al., 2014; Payandehjoo & Abhari, 2009, 2014; Qiu-Rong Zheng, Yun-Qi Fu, 2008; Radhi et al., 2019; Rajo-Iglesias et al., 2008; Sharma & Pandey, 2020; Shen et al., 2019; Soliman et al., 2015; Soukoulis, 2002; ; S. D. Assimonis et al., 2012; Suntives & Abhari, 2013; Tan et al., 2019; Thakur et al., 2020; Toolabi et al., 2016; W. Wu et al., 2018; Yablonovitch, 1987; X. M. Yang et al., 2012; A. Yu & Zhang, 2003);
Decoupling and Matching network	(Bilal et al., 2014; Cui et al., 2011; Gong et al., 2011; M. S. Khan et al., 2014; Lin et al., 2012; Malekpour & Honarvar, 2016; Moharram & Kishk, 2013; Piao et al., 2020; Radhi et al., 2018; Shabbir et al., 2020; T. C. Tang & Lin, 2014; Z. Tang et al., 2019; Xu et al., 2018, 2020; Xun et al., 2017; Jianfeng Zhu et al., 2017)
Neutralization line (NL)	(Asadpor & Rezvani, 2018; W. Jiang et al., 2019; Kayabasi et al., 2018; Liu, An, et al., 2020; Luo et al., 2019; Mondal et al., 2018; Ou et al., 2017; Saleh et al., 2017; Su & Lee, 2011; Tiwari, Singh, & Kanaujia, 2019; Tiwari, Singh, & Kanaujia, 2019; H. Wang et al., 2015; S. Wang & Du, 2015; Y. Wang & Du, 2014; Y. Yang et al., 2016; Y. Yu et al., 2016; Zhang & Pedersen, 2016)
Cloaking Structures	(Ahmed & Elwi, 2019; Alù & Engheta, 2005; Bernety & Yakovlev, 2015; Bisht et al., 2020; Z. H. Jiang et al., 2015; J. Li & Pendry, 2008; Moreno et al., 2016; Naqvi et al., 2016; Pendry et al., 2006; Jianfeng Zhu et al., 2016)
Shorting vias and pins	(Abdalla & Ibrahim, 2017; Abdullah et al., 2019; Aliakbari & Lau, 2020; Ling & Li, 2011; Park & Son, 2016; Singh et al., 2013; Sipal et al., 2019; Wong et al., 2017; Zaker, 2018)
Inherent or no isolation techniques	(Abed, 2018; Duan et al., 2019; Ekrami & Jam, 2018; Han et al., 2020; Jehangir & Sharawi, 2017; Jin et al., 2019; L. Liu et al., 2014; X. L. Liu et al., 2014; Malik et al., 2015; Sipal et al., 2018; Sun et al., 2020; H. Wang et al., 2015; S. M. Wang et al., 2015; Zhu & Eleftheriades, 2010)

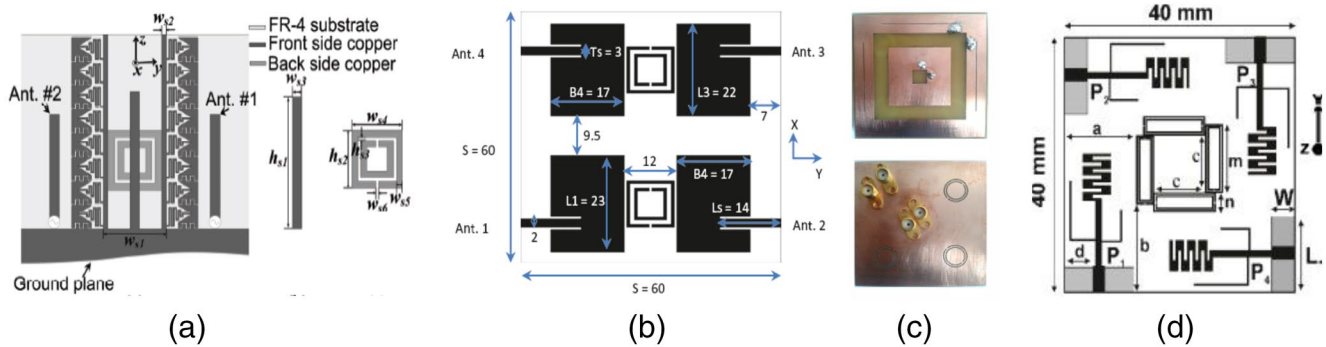


Figure 1. (a) Square SRR at the back (J. Y. Lee et al., 2015) (b) Pair of SRRs between the antenna (A. Kumar, Ansari, Kanaujia, & Kishor, 2018) (c) CSRRs loaded in its ground plane (Ramachandran et al., 2016) (d) A ring of four SRRs (Ramachandran et al., 2017). CSRR, complementary-split-ring-resonator; SRR, split-ring-resonator.

an array of 4×2 U-shaped slots resembling CSRRs structure (A. Kumar, Ansari, Kanaujia, Kishor, & Kandpal, 2018), slot combine CSRR on the surface as well as on the ground (Qamar et al., 2014; Shafique et al., 2015) as represented in Figure 3a, modified CSRR based MTM superstrate (Qamar et al., 2016), meta-structures consist π -shaped elements and capacitively grounded elements (M. C. Tang et al., 2017), a filter based on μ negative MTM (Thummaluru & Chaudhary, 2017) as represented in Figure 3b, MTM Labyrinth SRR (Torabi et al., 2016), as described in Figure 3c.

MTM isolator (F. Wang et al., 2018), compact SRR (Ntaikos & Yioultsis, 2013), a double layer MTM mushroom (Zhai et al., 2015), two arrays of square SRR on the top and one array of CSRR loaded ground (Öznazi & Ertürk, 2008), an array of SRRs and a metallic strip (Krishna et al., 2016) have been used to reduce the MC among elements of MIMO antenna. In some research, metasurface (Dadgarpour et al., 2017; Guo et al., 2019; G. C. Wu et al., 2015) has been used to reduce MC. MTM based FSS (Bilal et al., 2017; X. Zhu et al., 2017) has also been useful to minimize the MC.

From the comparison made in Table 2, it results that the MTMs help in achieving the isolation above 45 dB, better Envelop Correlation Coefficient (ECC), and works primarily for narrow-band MIMO antenna. MTMs generally require more area to be placed between the antenna's elements and mostly work in narrow-band antenna. MTMs are more useful in designing band-stop filters and achieving very high isolation among narrow-band MIMO antennas' elements.

One more thing we can observe that ECC calculated using S-parameters (A. Kumar, Ansari, Kanaujia, Kishor, et al., 2018) has lower values around 0.01 than the $ECC < 0.036$ calculated using far-field radiation pattern (A. Kumar et al., 2019). The far-field based computational ECC is more reliable as it considers

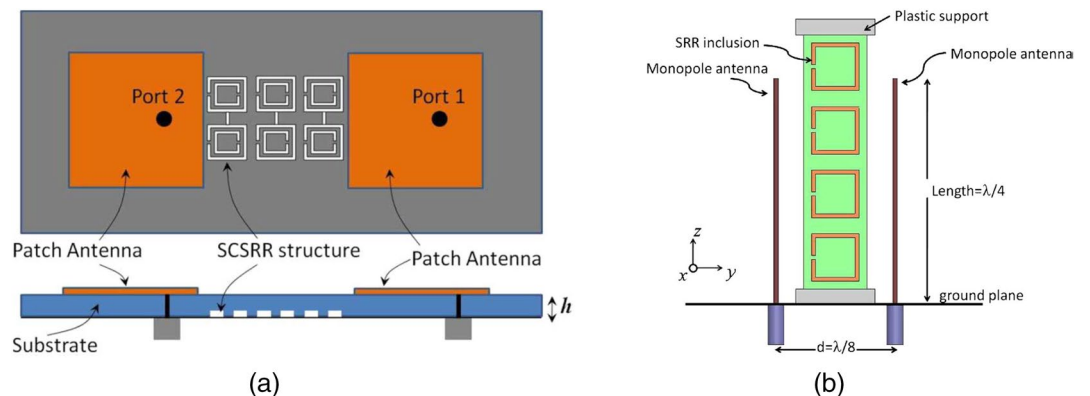


Figure 2. (a) Slotted CSRRs (Bait-Suwailam, Siddiqui, et al., 2010) (b) Single negative (MNG) MTMs (Bait-Suwailam, Boybay, et al., 2010). CSRR, complementary-split-ring-resonator; MTMs, Metamaterials.

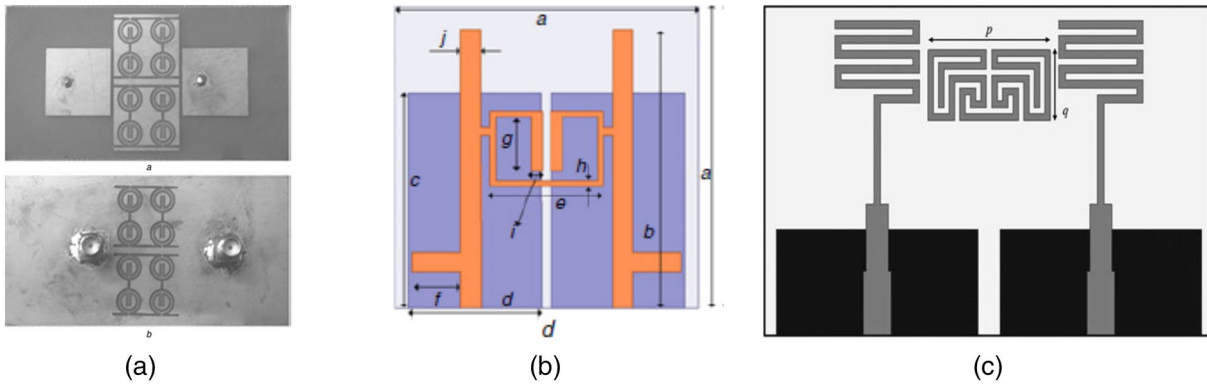


Figure 3. (a) Slot combine CSRR on surface and ground (Qamar et al., 2014) (b) μ negative MTM filter (Thummaluru & Chaudhary, 2017) (c) Labyrinth SRR (Torabi et al., 2016). CSRR, complementary-split-ring-resonator; MTM, Metamaterials.

the radiation pattern spatial diversity into consideration, unlike port isolation only in S-parameters-based computation.

2.2. Electromagnetic Band Gap Structures

EBG structures provide a high impedance path to surface wave propagation at specific operational frequencies and suppress the MC. EBG structures are periodic structures that avert or assist the propagation of electromagnetic waves in a specified band of frequencies irrespective of the angle of incident and polarization

Table 2
Comparison of MIMO Antenna Based on Metamaterials

Ref.	Substrate area ($l \times b$) $\text{mm}^2, \lambda_0 \times \lambda_0 = \lambda_0^2$	Min. isolation (dB)	Max. ECC value and computation approach	Type of metamaterials	No. of elements	Narrowband/Wideband/UWB
(A. Kumar, Ansari, Kanaujia, & Kishor, 2018)	$60 \times 60, 0.35 \times 0.35 = 0.12$	17	0.024, S-parameters	Pair of square SRR	4	Narrowband (Multi-band)
(J. Y. Lee et al., 2015)	$60 \times 57, 0.49 \times 0.46 = 0.23$	30	0.002, Far-field	1 D EBG and square SRR	2	Narrowband
(Ramachandran et al., 2016)	$60 \times 60, 0.49 \times 0.49 = 0.24$	22	0.4, Far-field	CSRRs loaded ground	4	Narrowband
(Ramachandran et al., 2017)	$40 \times 40, 0.26 \times 0.26 = 0.07$	22	0.3, Far-field	A ring of four SRRs	4	Multi-band
(Qamar et al., 2014)	$84 \times 44, 1.04 \times 0.54 = 0.56$	42	-	Slot combine CSRR on surface and ground	2	Narrowband
(Thummaluru & Chaudhary, 2017)	$45.5 \times 45.5, 0.40 \times 0.40 = 0.16$	35	~ 0 , S-parameters	μ negative MTM filter	2	Narrowband
(Torabi et al., 2016)	$24.3 \times 42.9, 0.19 \times 0.33 = 0.06$	45	0.0018, S-parameters	Labyrinth SRR	2	Narrowband
(Al-fayyadh & Alsabbagh, 2017)	$60 \times 60, 0.47 \times 0.47 = 0.22$	18	~ 0 , S-Parameters	A 3-D metamaterial structure	2	Narrowband
(Irene & Rajesh, 2018a)	$37 \times 44, 0.69 \times 0.82 = 0.57$	20	0.1, Far-field	Clip shaped MTM	2	Narrowband
(Zhai et al., 2015)	$119 \times 119, 0.96 \times 0.96 = 0.92$	42	0.02, Far-field	Double-layer mushroom structure	4	Narrowband

Abbreviations: CSRR, complementary-split-ring-resonator; EBG, electromagnetic band gap; ECC, envelop correlation coefficient; MIMO, multiple-input-multiple-output; MTM, Metamaterials; SRR, split-ring-resonator.

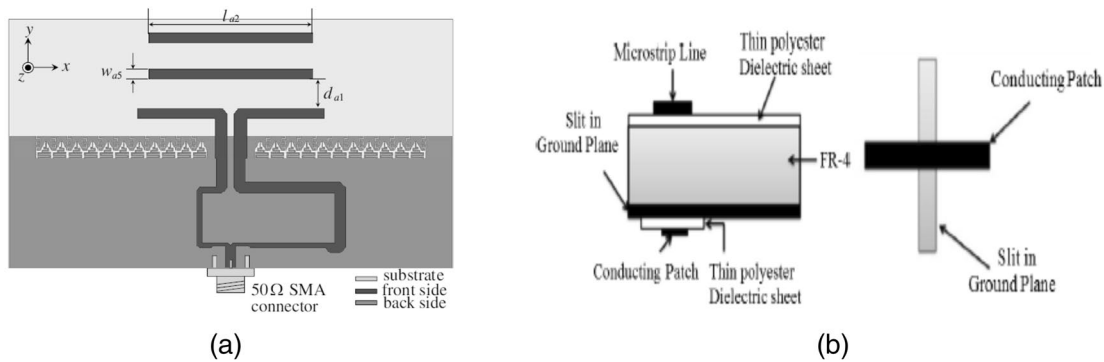


Figure 4. (a) 1-D EBG ground plane (Kim et al., 2011) (b) 2-D EBG comprises of patch and slit (Q. Li et al., 2014). EBG, electromagnetic band gap.

states of EM waves (Kapoor, 2013). EBG structures help in improving the radiation/gain patterns and decreasing the noise/losses in transmissions. The EBG structure concept has been originated by John (1987) and Yablonovitch (1987). When a bandgap or a frequency gap exists in a periodic dielectric substrate, then the EM wave with frequencies belonging to the gap cannot propagate in any direction inside the material. EBG structures may be formed on the metal or dielectric substrates and can be one dimensional (1-D), two dimensional (2-D), or three dimensional (3-D) depending upon the dimensions which satisfy the Bragg's conditions, which states that the inter-cell separation (period) is close to half guided wavelength ($\lambda_g/2$) and are capable of averting EM propagation in either all or selected directions (J. D. Shumpert, et al., 1997; Soukoulis, 2002).

A dipole antenna designed with the 1-D EBG ground plane, as represented in Figure 4a, has higher directivity and a better FB (front-to-back) ratio (Kim et al., 2011). While 1-D EBG structure, inserted between two closely located monopole antenna, has suppressed MC (J. Y. Lee et al., 2015). A planar EBG structure has been printed on the high permittivity substrate in a multilayer patch antenna for suppressing MC (Rajo-Iglesias et al., 2008). A 2-D EBG structure employs two tightly coupled arrays, one comprising of conducting patch. The other is the slits in the ground plane as represented in Figure 4b to reduce the MC between two monopoles UWB-MIMO antenna (Q. Li et al., 2014). Similarly, many EBG structures have been studied in the literature, among them, few are going to be discussed here: 1-D EBG structure comprises of patterns of grids on the top patch with a metallic ground plane, and both are shorted by several vias (W. Wu et al., 2018); conventional mushroom EBG structure loaded with slots (Lu & Lin, 2013); 4×1 array configuration of a unit cell size (6.8×6.8 mm) unipolar EBG (Dabas et al., 2018); multi-layered EBG structure (T. Jiang et al., 2018); a novel uni-conductor EBG placed between patch antenna as represented in the Figure 5a (Mohamed et al., 2019); EBG structure based on MTM (Alibakhshikenari et al., 2019b); waveguided MTM realized by crossed-meander-line slits exhibit magnetic resonance as well as the band-gap property (X. M. Yang et al., 2012); another EBG ground structure can be viewed in Figure 5b (Shen

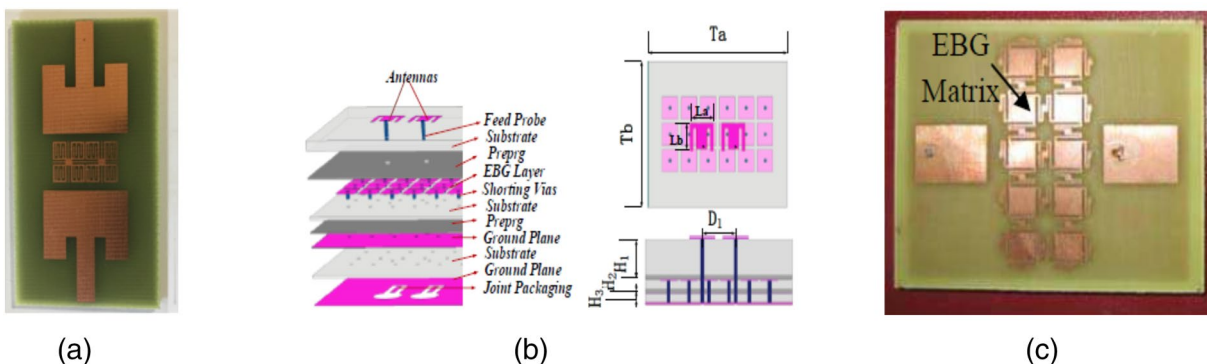


Figure 5. (a) A novel uni-conductor EBG placed between patch antenna (Mohamed et al., 2019) (b) a novel EBG ground (Shen et al., 2019) (c) 2×5 EBG structure (Islam & Alam, 2013). EBG, electromagnetic band gap.

Table 3
Comparison of MIMO Antenna Based on EBG

Ref.	Substrate area ($1 \times b$) mm^2 , $\lambda_0 \times \lambda_0 = \lambda_0^2$	Min. Isolation (dB)	Max. ECC value and computation approach	Type of EBG	No. of elements	Narrowband/ Wideband/ UWB
(Q. Q. Li et al., 2014)	50×60 , $0.50 \times 0.50 = 0.25$	13	–, –	2-D EBG comprises of patch and slit	2	Wideband
(W. W. Wu et al., 2018)	60×60 , $0.60 \times 0.60 = 0.36$	17.5	0.3, Far-field	Patterns of grids shorted to the ground plane through vias	4	UWB
(Dabas et al., 2018)	27.2×46 , $0.27 \times 0.46 = 0.12$	18	0.018, S-parameters	Uniplanar EBG	2	UWB
(Mohamed et al., 2019)	49×24 , $0.95 \times 0.46 = 0.44$	35	0.03, Far-field	Novel uni-conductor EBG	2	Narrowband
(Alibakhshikenari et al., 2019b)	37×70 , $1.07 \times 2.03 = 2.17$	20	–, –	EM-Bandgap Metamaterial Fractal Loading	2	Wideband (Multi-band)
(X. M. X. M. Yang et al., 2012)	76.4×91 , $0.78 \times 0.93 = 0.73$	16	–, –	Crossed-meander-line slits	2	Narrowband
(Tan et al., 2019)	44×58 , $0.50 \times 0.66 = 0.33$	26	0.089, Far-field	Split Uniplanar EBG	2	Narrowband (Multi-band)
(Al-Fayyadh et al., 2017)	34.5×60 , $0.40 \times 0.70 = 0.28$	21.6	0.001, S-parameters	Uniplanar EBG	2	Narrowband
(Mohamadzade & Afsahi, 2017)	45×90 , $0.84 \times 1.68 = 1.41$	33.06	–	4×2 Compact EBG cells	2	Narrowband
(Radhi et al., 2019)	68×40 , $0.60 \times 0.35 = 0.21$	27	0.0003, S-parameters	Fractal based EBG	2	Narrowband

Abbreviations: EBG, electromagnetic band gap; ECC, envelop correlation coefficient; MIMO, multiple-input-multiple-output.

et al., 2019); a 2×5 EBG structure as represented in Figure 5c (Islam & Alam, 2013); split EBG structure (Tan et al., 2019); a novel and compact spiral EBG (Qiu-Rong Zheng, Yun-Qi Fu, 2008); EBG based corrugated structure (Lu & Lin, 2013); Tunable Double-Layer EBG structures (Mavridou et al., 2016); some famous uniplanar EBG structure (Abedin & Ali, 2005; Abidin et al., 2018; Al-Fayyadh et al., 2017; Alibakhshikenari, Virdee, et al., 2018; Farahani et al., 2010; Iqbal et al., 2019; Mohamadzade & Afsahi, 2017; Mu'ath J et al., 2014; Payandehjoo & Abhari, 2009; Soliman et al., 2015; Toolabi et al., 2016); dumbbell-shaped EBG structure (A. Yu & Zhang, 2003); electromagnetic soft surfaces realized by metal strips loaded with C-shaped slots (Chen et al., 2018); multilayer EBG structure (Exposito-Dominguez et al., 2012); MTM inspired EBG structure (Alibakhshikenari et al., 2019a) mushroom type EBG structure (J. Kumar, 2016); high impedance ground plane (Y. Lee & Sun, 2008); multilayer mushroom type EBG (Payandehjoo & Abhari, 2014); EBG structure introduced at superstrate level (Suntives & Abhari, 2013) and a novel Fractal based uniplanar EBG (Radhi et al., 2019) have been used to suppress the surface wave propagation hence reduce the MC among microstrip antennas. Many more EBG structures and their optimization have been discussed in Alam et al. (2013) and S. D. Assimonis et al. (2012) and Ebadi and Semnani (2014).

Table 3 indicates that EBG based MIMO antennas are generally bulky, and EBG structures help minimize the MC for MIMO antennas working in a specific range. Uniplanar EBG structures were the most common of all the designs.

2.3. Decoupling and Matching Network

Sometimes decoupled and matched network between the patch antenna helps to cater away the coupled field and hence suppress the MC. Two π -shaped decoupling strip structures were introduced between the patch antenna to suppress the MC (J. Zhu et al., 2017). Xun et al. have used a compact planar spiral line structure to decouple the MC, as represented in Figure 6a (Xun et al., 2017). A decoupling structure comprised metalized via walls, and short-circuited stepped-impedance designs have been used to suppress MC (K. Da Xu et al., 2018) as represented in Figure 6b. A decoupling path is provided by the strips which are

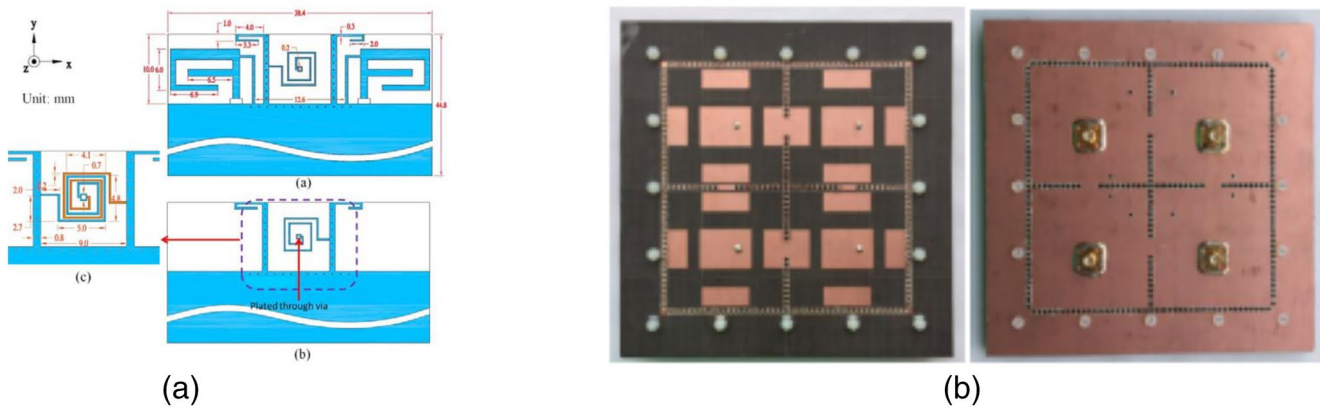


Figure 6. (a) Compact planar spiral line (PSL) structure (Xun et al., 2017) (b) metalized via walls and short-circuited stepped-impedance structures (K. Da Xu et al., 2018).

placed beneath the patch antenna and are shorted by the vias (T. C. Tang & Lin, 2014). Some parasitic type-decoupling structures like a floating parasitic digitated decoupling structure (M. S. Khan et al., 2014), a comb-like decoupling structure on the ground plane (Malekpour & Honarvar, 2016) and a novel decoupling structure (Radhi et al., 2018) as represented in Figures 7a–7c respectively have been used for reducing the MC.

A novel and general decoupling network has been proposed using a single transmission line connected between the input ports of the antenna (Moharram & Kishk, 2013), as represented in Figure 8a. A sinusoidal decoupling structure (Bilal et al., 2014) and a novel decoupling along with DGS, slots, and slits (Z. Tang et al., 2019) have been used in a UWB-MIMO antenna as represented in Figures 8b and 8c, respectively.

Two transmission lines (TLs) are connected to two closely spaced antennas. Their lengths are designed so that the trans-admittance between the port changes from complex to imaginary only. A reactive shunt component is then attached to cancel the imaginary part and cancels any coupling between the antenna (Lin et al., 2012) as represented in Figure 9a. In another case, a decoupling network has been assigned between the antenna along with a slot cut in the ground plane (Cui et al., 2011) while, in another example, a hybrid ring of arbitrary power division has been implemented as an orthogonal feeding network (Gong et al., 2011) as represented in Figures 9b and 9c, respectively, to improve the isolation between the two monopole antennas.

As shown in Table 4, the decoupling and matching network is ideally suitable for narrow-band MIMO antenna with the compactness of around $0.06 \lambda_0^2$ (Cui et al., 2011). Although the authors claim in some of the proposed works (Bilal et al., 2014; M. S. Khan et al., 2014; Malekpour & Honarvar, 2016; Radhi et al., 2018; Z. Tang et al., 2019) as decoupling isolation structure but the MIMO antenna having a decoupling network

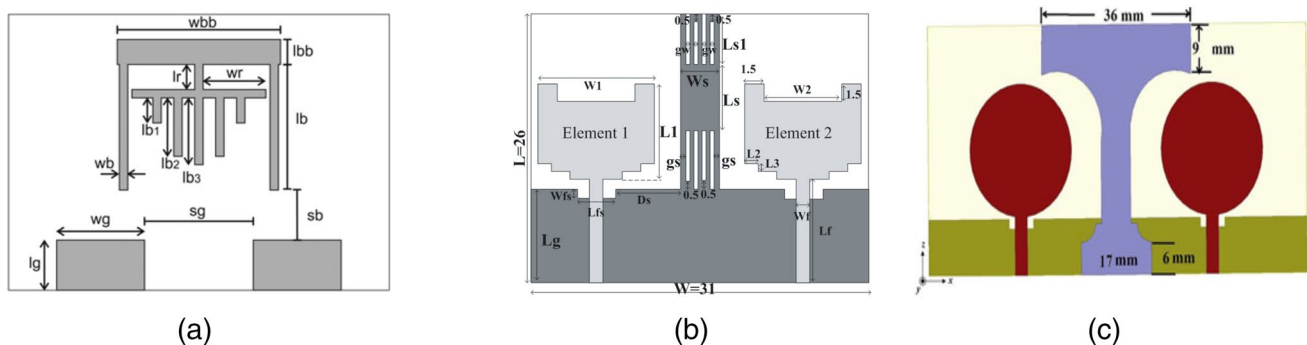


Figure 7. (a) Floating parasitic structure (M. S. Khan et al., 2014) (b) comb-like (Malekpour & Honarvar, 2016) (c) partial ground (Radhi et al., 2018).

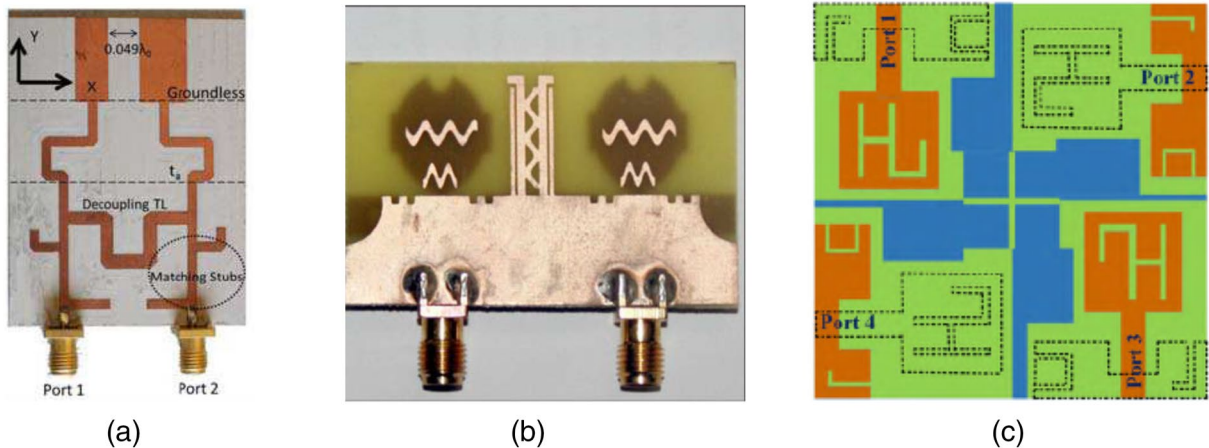


Figure 8. (a) A novel and general decoupling network (Moharram & Kishk, 2013) (b) sinusoidal decoupling structure (Bilal et al., 2014) (c) a novel decoupling structure along with DGS, slots & slits (Z. Tang et al., 2019). DGS, defected ground structures.

is more like parasitic structure, protruding ground stub and slots/slits-etching which results in high isolation among the compact UWB-MIMO antenna.

2.4. Neutralization Line

Neutralization line (NL) is one of the unconventional techniques popular because of its simplicity and compactness, which suppresses the MC. Unlike the parasitic elements/structures, NL feeds the passive antenna with the EM wave of the same phase, which NL receives from the active antenna to cancel out the EM signal, induced from the active to the passive antenna. Always a low impedance area of the antenna is preferred to connect the NL.

Along with four cuts on the ground, the NL connecting both the symmetrical radiating element (Y. Yang et al., 2016), as represented in Figure 10a, helps minimize the MC. A similar structure of NL likes above, but now with a matrix of 3×3 CSRRs loaded ground (Asadpor & Rezvani, 2018) has been used for MC reduction.

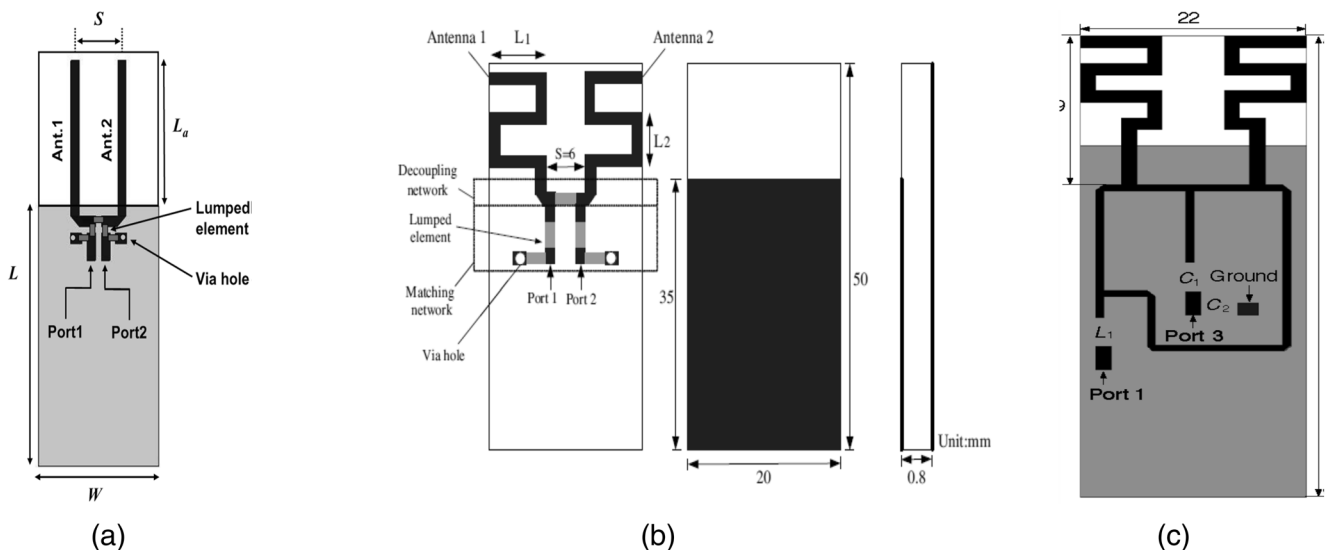


Figure 9. (a) Two TLs with reactive shunt component (Lin et al., 2012) (b) decoupling network along with a lumped element (Cui et al., 2011) (c) hybrid ring of arbitrary power division (Gong et al., 2011).

Table 4
Comparison of MIMO Antenna Based on Decoupling and Matching Network

Ref.	Substrate area ($l \times b$) mm^2 , $\lambda_0 \times \lambda_0 = \lambda_0^2$	Min. Isolation (dB)	Max. ECC value and computation approach	Type of network	No. of elements	Narrowband/Wideband/UWB
(Xun et al., 2017)	44.8×38.4 , $0.36 \times 0.31 = 0.11$	20.3	–	Compact planar spiral line (PSL) structure	2	Narrowband (Multi-band)
(K. Da Xu et al., 2018)	160×160 , $1.79 \times 1.79 = 3.20$	28	–	Metalized via walls and short-circuited stepped-impedance structures	4	Narrowband
(M. S. Khan et al., 2014)	33×45.5 , $0.34 \times 0.47 = 0.16$	20	0.3, Far-field	Floating parasitic digitated decoupling structure	2	UWB
(Malekpour & Honarvar, 2016)	26×31 , $0.27 \times 0.32 = 0.09$	25	0.001, S-parameters	Comb-like decoupling structure	2	UWB
(Radhi et al., 2018)	47×93 , $0.49 \times 0.96 = 0.47$	31	0.035, S-parameters	Wideband planar decoupling structure	2	UWB
(Moharram & Kishk, 2013)	42×45 , $0.34 \times 0.37 = 0.13$	15	~ 0 , S-parameters/Far-field	Inverted ohm-shaped connecting transmission line	2	Narrowband
(Bilal et al., 2014)	30×50.5 , $0.30 \times 0.51 = 0.15$	20	0.53, S-parameters	Sinusoidal Decoupling Structure	2	UWB
(Z. Z. Tang et al., 2019)	39×39 , $0.30 \times 0.30 = 0.09$	22	0.02, Far-field	A novel decoupling structure along with DGS, slots & slits	2	UWB
(Lin et al., 2012)	45×22 , $0.37 \times 0.18 = 0.07$	20	–	Two TLs with shunt reactive component	2	Narrowband
(Cui et al., 2011)	50×20 , $0.40 \times 0.16 = 0.06$	35	0.1, S-parameters	Decoupling network along with a lumped element	2	Narrowband
(Gong et al., 2011)	70×22 , $0.56 \times 0.18 = 0.10$	23	0.1, S-parameters	Hybrid ring of arbitrary power division	2	Narrowband

Abbreviations: ECC, envelop correlation coefficient; MIMO, multiple-input-multiple-output.

A wideband NL comprises two metal strips and one circular disc (Zhang & Pedersen, 2016), as represented in Figure 10b; the circular disc provides multiple decoupling current paths that help achieve wideband decoupling. A simple meandered-shaped metallic stripline (Y. Yu et al., 2016) has been used as NL to cancel coupling between circular rings shaped radiating patch antennas as represented in Figure 11a. An NL comprises two metallic strips and a rectangular patch (Tiwari, Singh, & Kanaujia, 2019; Tiwari, Singh, & Kanaujia, 2019), as described in Figure 11b has been used between the UWB-MIMO antenna elements. A simple metallic strip was connecting the feedline (Luo et al., 2019; Ou et al., 2017); triple branch NL along

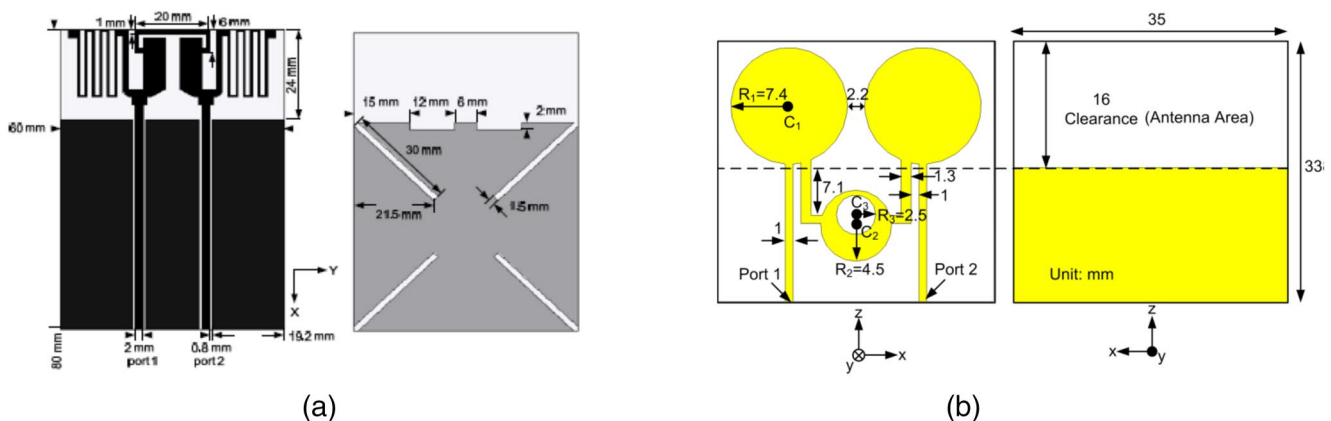


Figure 10. (a) NL along with four cuts in the ground plane (Y. Yang et al., 2016) (b) NL comprises two metal strips and one circular disc (Zhang & Pedersen, 2016). NL, neutralization line.

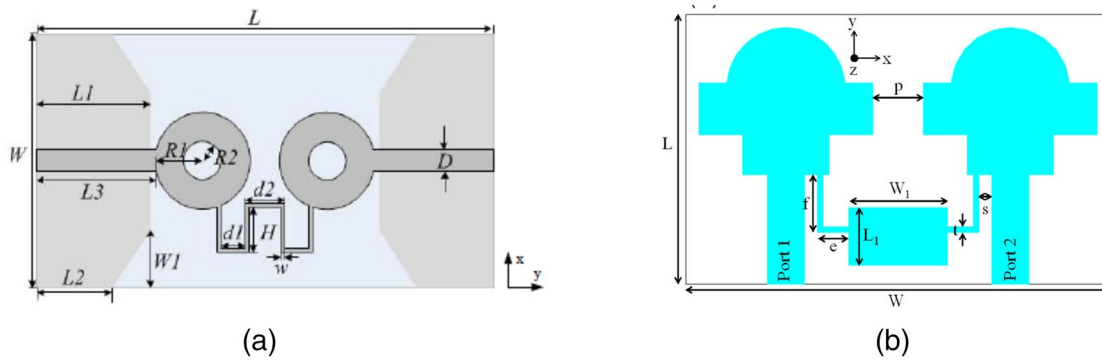


Figure 11. (a) Meandered-shaped metallic NL (Y. Yu et al., 2016) (b) NL comprises of two metallic strips and a rectangular patch (Tiwari, Singh, & Kanaujia, 2019; Tiwari, Singh, & Kanaujia, 2019). NL, neutralization line.

with DGS (Mondal et al., 2018), as represented in Figure 12a; a microstrip neutralization network (H. Wang et al., 2014) as depicted in Figure 12b; NL along with inverted I-ground slots (W. Jiang et al., 2019); a simple NL connecting the ground of CPW-Fed tri-band MIMO antenna (Saleh et al., 2017); crossed NL (S. Wang & Du, 2015); typical NL (Su & Lee, 2011); a neutralization ring (Kayabasi et al., 2018) and a group of three NLs (Y. Wang & Du, 2014) have been used to cancel the coupling from one antenna to another radiating patch antenna.

Table 5 represents that just like parasitic structures, NLs are useful for all the cases: narrow-band, wideband, UWB-MIMO antennas.

2.5. Cloaking Structures

This method deals with electromagnetic invisibility where the bistatic scattering width of a given object is suppressed independent of the angle of incidence and observations.

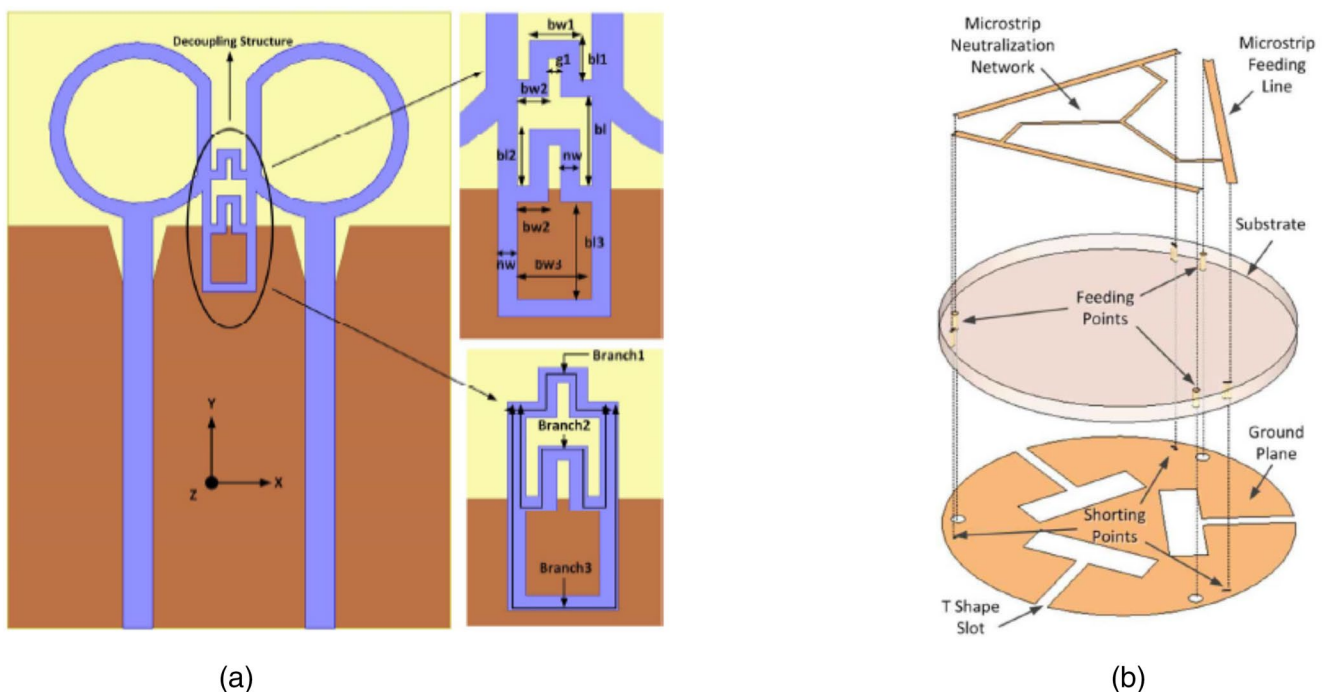


Figure 12. (a) Triple branch NL along with DGS (Mondal et al., 2018) (b) microstrip neutralization network (H. Wang et al., 2014). DGS, defected ground structures; NL, neutralization line.

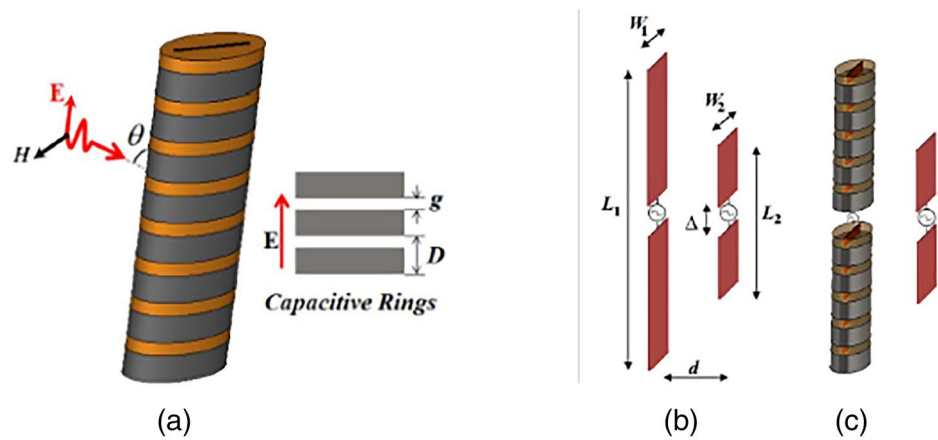
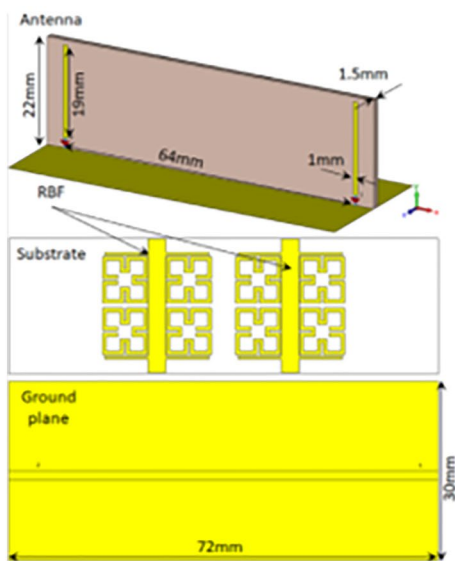


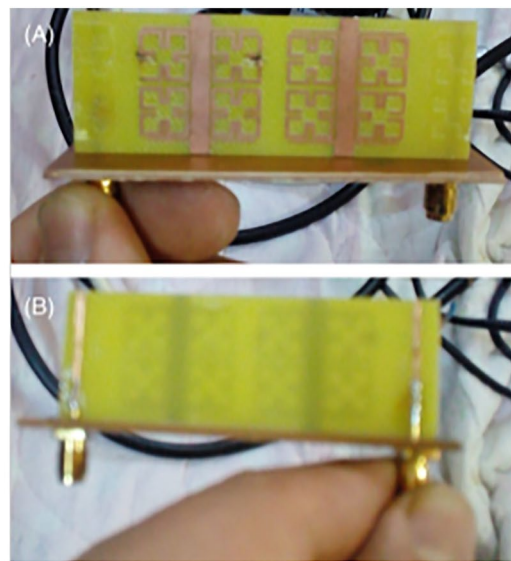
Figure 13. (a) Confocal elliptical metasurface cloaks (b) Two strip dipole antenna (c) One strip dipole cloaked from another (Bernety & Yakovlev, 2015).

Some cloaked structures are based on the principle of bending EM waves around the object (J. Li & Pendry, 2008; Pendry et al., 2006) to be cloaked, while in some cases, bulk isotropic low or negative index materials (Alù & Engheta, 2005) is used to suppress the dominant scattering mode. The confocal elliptical metasurface consists of periodic sub-wavelength elements (Bernety & Yakovlev, 2015) used to cloak the one strip dipole antenna from the firmly placed other dipole antenna as represented in Figure 13a-13c. The similar design process of cloaking one strip dipole antenna from another has been followed at terahertz frequencies with an elliptically shaped graphene monolayer (Moreno et al., 2016).

Two reject band filter (RBF) cells placed adjacently have resulted in a zero refractive index at 2.5 GHz (Ahmed & Elwi, 2019), as represented in Figure 14a-14b and thus suppressing the MC between monopole antennas. The use of metasurfaces, which is quasi-2D, which consists of arrays of the sub-wavelength environment (Z. H. Jiang et al., 2015), as represented in Figure 15, exhibits dispersive properties.



(a)



(b)

Figure 14. (a) Designed two RBF (b) Fabricated monopole MIMO antenna with the two RBF (Ahmed & Elwi, 2019). MIMO, multiple-input-multiple-output; RBF, reject band filter.

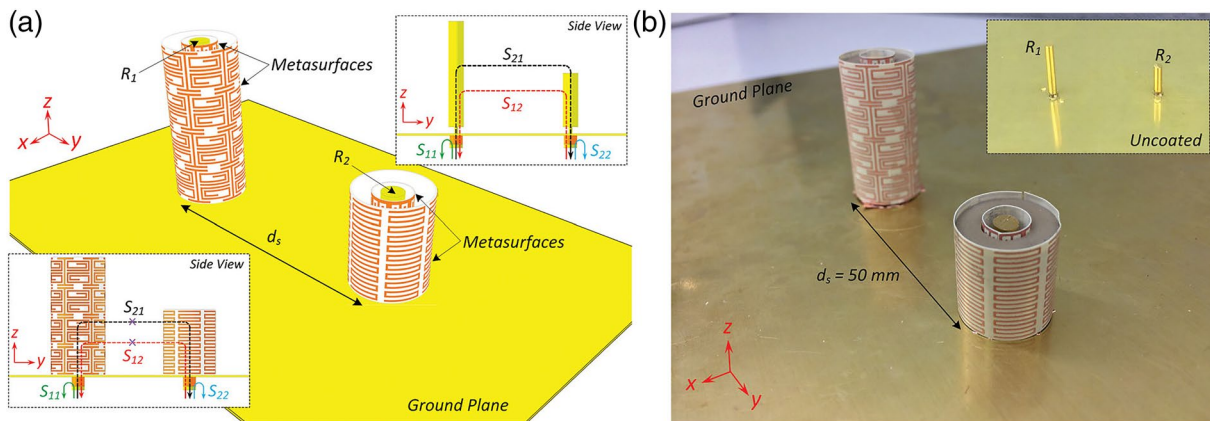


Figure 15. Quasi-2D functional metasurfaces (Z. H. Jiang et al., 2015).

In another case, the cylindrical-shaped cloaking-based surface comprises several interconnected 2-port microstrips (2-PM) (Jianfeng. Zhu et al., 2016), and interconnected 2-port reconfigurable microstrip (2-PFRM) (Naqvi et al., 2016) have been illustrated in Figures 16a and 16b, respectively, which helps in reducing MC.

Table 5
Comparison of MIMO Antenna Based on NL

Ref.	Substrate area ($1 \times b$) $\text{mm}^2, \lambda_0 \times \lambda_0 = \lambda_0^2$	Min. Isolation (dB)	Max. ECC value and computation approach	Type of NL	No. of elements	Narrowband/Wideband/Multi-band/UWB
(Y. Y. Yang et al., 2016)	$80 \times 60, 0.24 \times 0.18 = 0.04$	30	–	Simple rectangular NL	2	Narrowband (Multi-band)
(Zhang & Pedersen, 2016)	$33 \times 35, 0.31 \times 0.36 = 0.11$	22	0.1, Far-field	NL comprises two metal strips and one circular disc	2	Wideband
(Y. Yu et al., 2016)	$40 \times 80, 0.41 \times 0.83 = 0.34$	15	–	Meandered-shaped metallic NL	2	UWB
(Tiwari, Singh, & Kanaujia, 2019)	$21 \times 34, 0.25 \times 0.40 = 0.10$	22	0.005, S-parameters	NL comprises of two metallic strips and a rectangular patch	2	UWB
(Ou et al., 2017)	$50 \times 40, 0.41 \times 0.33 = 0.14$	20	0.005, S-parameters	Simple metallic strip connecting the feedline	2	Narrowband (Multi-band)
(Mondal et al., 2018)	$22 \times 15, 0.65 \times 0.45 = 0.30$	20	0.001, S-parameters	Triple branch NL	2	Wideband
(H. Wang et al., 2014)	$\pi 16 \times 16, 0.40 \times 0.13 = 0.05$	15	0.029, Far-field	Microstrip neutralization network	3	Narrowband
(W. Jiang et al., 2019)	$124 \times 74, 1.36 \times 0.81 = 1.10$	15	0.15, Far-field	Simple Rectangular NL	8	Narrowband
(Saleh et al., 2017)	$36 \times 47, 0.29 \times 0.38 = 0.11$	18	0.08, S-parameters	Simple Rectangular NL	2	Wideband (Multi-band)
(S. Wang & Du, 2015)	$135 \times 80, 0.34 \times 0.20 = 0.07$	10	0.283, Far-field	Crossed NL	2	Narrowband (Multi-band)
(Su & Lee, 2011)	$65 \times 35, 0.52 \times 0.28 = 0.15$	18	–	Normal NL	2	Narrowband
(Kayabasi et al., 2018)	$75.19 \times 75.19, 0.78 \times 0.78 = 0.61$	13	0.1, –	Neutralization ring	4	UWB
(Y. Wang & Du, 2014)	$115 \times 60, 0.62 \times 0.32 = 0.20$	15	0.053, S-parameters	Three NLs	2	Wideband

Abbreviations: ECC, envelop correlation coefficient; MIMO, multiple-input-multiple-output; NL, neutralization line.



Figure 16. Cylindrical cloaking surface (a) interconnected 2-port microstrip (2-PM) (Jianfeng. Zhu et al., 2016) (b) interconnected 2-port reconfigurable microstrip (2-PFRM) (Naqvi et al., 2016).

2.6. Shorting Vias and Pins

Another prevalent method is shorting any parasitic elements/structures through metallic vias and pins to provide an additional decoupling path for the coupled fields before it reaches the other antenna placed in closer proximity. Six metallic pins (Abdullah et al., 2019) have been shorted near the adjacent edges of a square patch antenna to its ground, as represented in Figure 17a, to minimize the MC. In another case, a folded shorting strip (Singh et al., 2013) has been attached to each of the two-port antennae to enhance the port-to-port isolation. A simple metallic strip and shorting vias (Sipal et al., 2019), as represented in Figure 17b, have been used to counter MC. Similarly, two stubs as shunt inductor (Abdalla & Ibrahim, 2017), H-shaped conducting wall shorted by vias (Park & Son, 2016), a shorting strip and isolation stub (Ling & Li, 2011), a pair of novel shorted inverted L-shaped strips (Zaker, 2018) and two shorted strip between two gap-coupled loop antennas (Wong et al., 2017) have been used to provide an additional path to the coupled fields and hence reduces the MC.

It can be observed from Table 6 that the shorting vias and pins work mainly in narrow-band MIMO antenna for achieving high isolation. It means, if high isolation in a narrow-band compact MIMO antenna is targeted, then shorting vias and pins is one of the best techniques.

Table 6
Comparison of MIMO Antenna Based on Shorting Vias and Pins

Ref.	Substrate area ($1 \times b$) mm^2 , $\lambda_0 \times \lambda_0 = \lambda_0^2$	Min. Isolation (dB)	Max. ECC value and computation approach	Type	No. of elements	Narrowband/ Wideband/ Multi-band/UWB
(Abdullah et al., 2019)	30×55 , $0.35 \times 0.64 = 0.22$	20	0.01, Far-field	Pair of shorted six metallic pins	2	Narrowband
(Singh et al., 2013)	110×60 , $0.88 \times 0.48 = 0.42$	26	0.01, Far-field	Folded shorting strip	2	Narrowband (Dual-band)
(Sipal et al., 2019)	42×38 , $0.32 \times 0.25 = 0.08$	20	0.05, Far-field	Metallic strip along with shorting vias	2	Narrowband (Dual-band)
(Abdalla & Ibrahim, 2017)	26×30 , $0.50 \times 0.58 = 0.29$	45	0.0002, S-parameters	Two stubs as shunt inductor	2	Narrowband
(Park & Son, 2016)	30×50 , $0.52 \times 0.87 = 0.45$	51	–	H-shaped conducting wall shorted by vias	2	Narrowband
(Ling & Li, 2011)	50×15 , $0.40 \times 0.12 = 0.05$	20	0.01, S-parameters	Shorting strip and isolation stub	2	Narrowband (Dual-band)
(Zaker, 2018)	–	58	0.1, Far-field	A pair of novel shorted inverted L-shaped strips	2	Narrowband
(Wong et al., 2017)	150×75 , $1.7 \times 0.85 = 1.46$	–	0.1	Two shorted strip between two gap-coupled loop antennas	8	Narrowband

Abbreviation: MIMO, multiple-input-multiple-output.

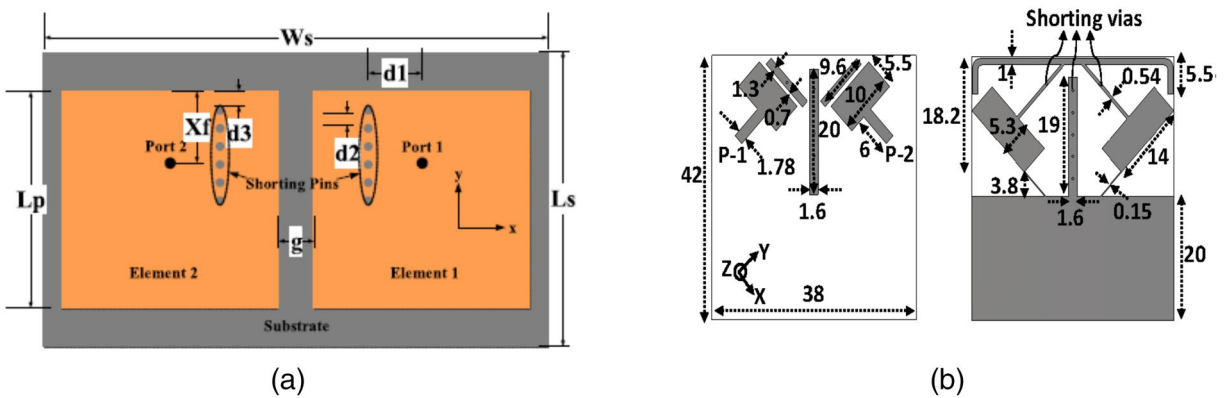


Figure 17. (a) Six pairs of shunting vias (Abdullah et al., 2019) (b) metallic strip along with shunting vias (Sipal et al., 2019).

2.7. Inherent or No Isolation Techniques

Sometimes the designed MIMO antenna has inherent characteristics to counter the MC induced from one antenna to another, like in few cases of the quasi self-complementary antenna (QSCA). While in some cases, the pattern diversity due to the unique design style gives us the privilege of no requirement of additional decoupling mechanisms to enhance the isolation. However, the significant disadvantages of such kind of structure are the increased space requirement between the elements of the MIMO antenna. Two coupled feed MIMO antennas have broad impedance matching bands, separated by a small gap that has a built-in isolation mechanism, due to the opposite currents generated at the edges of the circular pads and the feeds (S. M. Wang et al., 2015) as represented in Figure 18a-18b. A semi-ring slot Yagi-like MIMO antenna (Jehangir & Sharawi, 2017) with a compact complementary slot reflector element has been proposed without having a specific decoupling structure for MC reduction. Similarly, many designs have been reported in the literature (Abed, 2018; Duan et al., 2019; Ekrami & Jam, 2018; Jin et al., 2019; Malik et al., 2015; Sipal et al., 2018), which does not require any additional decoupling mechanism/structure to achieve the necessary isolation. Self-decoupled X-shaped arms etched on the square-shaped substrate (H. Wang et al., 2015) as represented in Figure 19a will show ultra-high isolation having orthogonal modes while in another case, two MTM-inspired monopole antennas (Jiang, Zhu & Eleftheriades, 2010) have reduced MC because of self-cancellation of the induced common ground and near field currents without requiring any additional decoupling mechanism as represented in Figure 19b.

QSCA designs are favorable to the UWB-MIMO antenna proposal because of their wide impedance matching capability and no requirement of an additional decoupling mechanism for having sufficient isolation (L. Liu et al., 2014; X. L. Liu et al., 2014). Two such QSCA designs have been shown in Figures 20a and 20b.

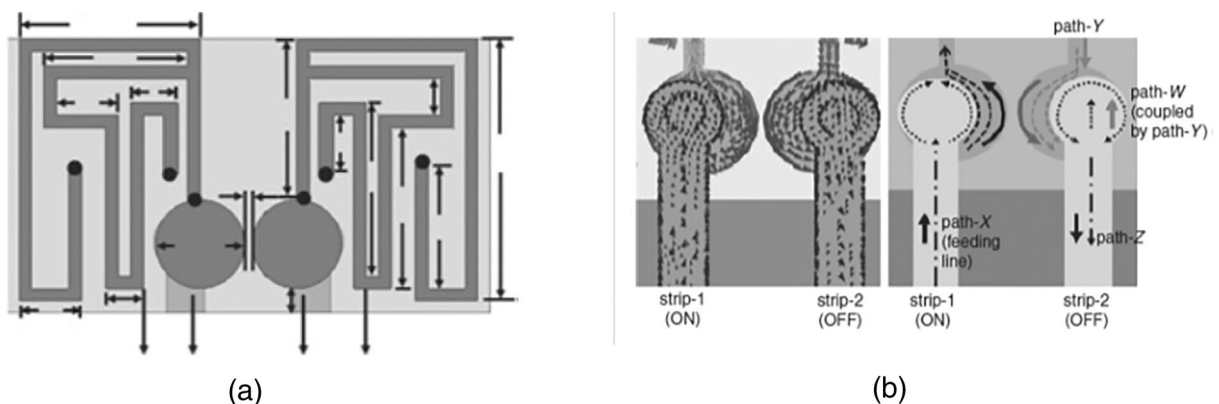


Figure 18. (a) Couple feed MIMO antenna (b) current distribution along the circular edge and feeds (S. M. Wang et al., 2015). MIMO, multiple-input-multiple-output.

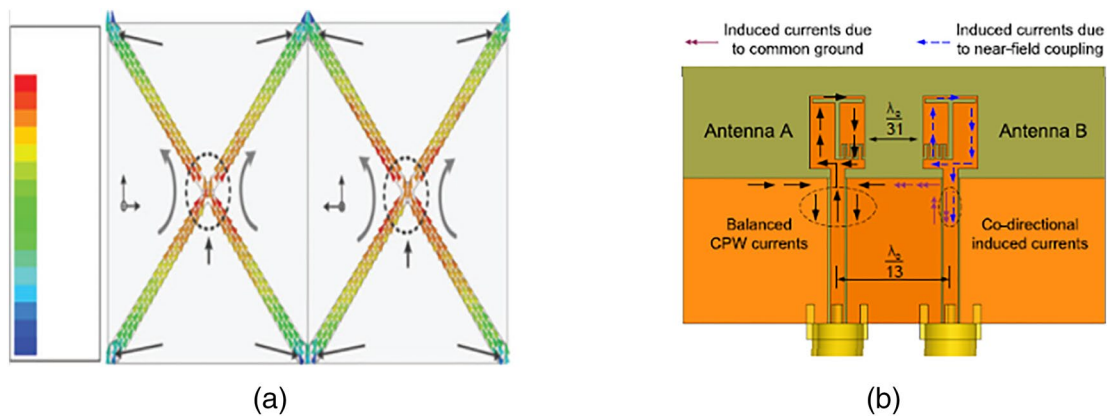


Figure 19. (a) X-shaped etched arms (H. Wang et al., 2015) (b) MTM-inspired MIMO antenna (Jiang, Zhu & Eleftheriades, 2010). MIMO, multiple-input-multiple-output; MTM, Metamaterials.

Therefore, we have discussed various existing literature methods for minimizing the MC among the MIMO antenna elements.

3. Conclusions and Future Scope

In all the above cases, it has been found that the isolation or suppressing of MC is a significant problem in the lower frequency range as the λ increases with the decrease of the frequency. It has been observed throughout that the ECC calculated from far-field radiation patterns will have higher values than the one calculated from S-parameters. Protruding Ground Stubs, DGSs, Slots/Slits-etching, and Parasitic Elements/Structures are widely suitable for reducing MC in wideband and UWB-MIMO antennas as discussed in part one of this two-part article. Whereas MTMs, EBG, and Shorting Pins/Vias are more useful in lowering MC among elements of narrow-band MIMO antenna.

There is plenty of room in the future to extend the research. Some possible solutions are mentioned below:

- the use of other expensive lossless substrates as compared to the lossy inexpensive FR-4 one for better efficiency and gain
- till now, the study focused mainly on 2×2 or 4×4 MIMO antenna design. Massive MIMO can be designed for future wireless communications which will have at least eight antenna elements which will further increase the data throughput without sacrificing additional spectrum
- fractal geometry-based MIMO antenna isolated with the help of EBG or Metamaterials can be proposed and designed

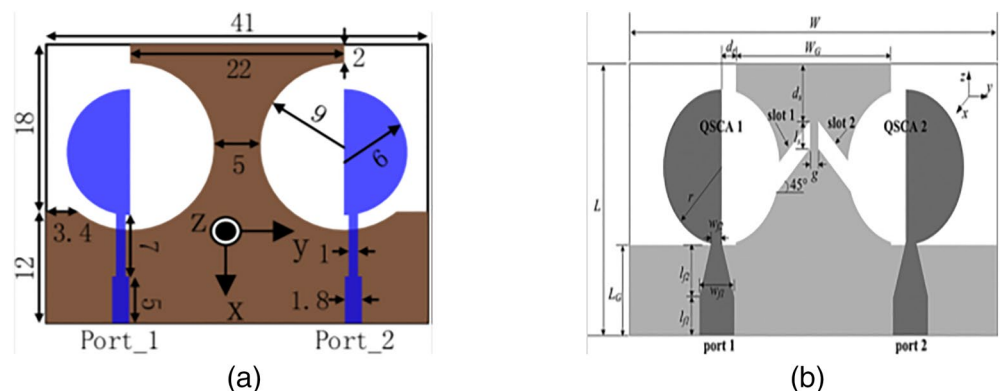


Figure 20. (a) QSCA (L. Liu et al., 2014) (b) QSCA with a minor defect in the ground (L. Liu et al., 2014). QSCA, quasi self-complementary antenna.

- d) tunable MIMO antenna with reduced MC will give an immense scope of research
- e) tunable isolation structure as per the required operating frequency range, like overlapping of SRRs of different dimensions and their switching with the help of varactor diodes, will be of great help
- f) designing of MIMO antenna having zeroth-order resonance with high isolation

Data Availability Statement

It is a review article. All the particulars like content, Figures, taken from other articles are specifically cited on all occasions. Rest everything are contributed by the authors only.

Acknowledgment

The authors acknowledge the CRS project having Application ID: 1-5748389248 sanctioned under TEQIP-III by the National Project Implementation Unit (NPIU), a unit of Ministry of Human Resource Development (MHRD), Government of India.

References

- Abdalla, M. A., & Ibrahim, A. A. (2017). Design and performance evaluation of metamaterial inspired MIMO antennas for wireless applications. *Wireless Personal Communications*, 95(2), 1001–1017. <https://doi.org/10.1007/s11277-016-3809-4>
- Abdelgwad, A. H., & Ali, M. (2020). Isolation improvement of a two-port PIFA for MIMO using a planar EBG ground. *Microwave and Optical Technology Letters*, 62(2), 737–742. <https://doi.org/10.1002/mop.32059>
- Abdullah, M., Li, Q., Xue, W., Peng, G., He, Y., & Chen, X. (2019). Isolation enhancement of MIMO antennas using shorting pins. *Journal of Electromagnetic Waves and Applications*, 33(10), 1249–1263. <https://doi.org/10.1080/09205071.2019.1606738>
- Abed, A. T. (2018). Highly compact size serpentine-shaped multiple-input-multiple-output fractal antenna with CP diversity. *IET Microwaves, Antennas & Propagation*, 12(4), 636–640. <https://doi.org/10.1049/iet-map.2017.0770>
- Abedin, M. F., & Ali, M. (2005). Effects of a smaller unit cell planar EBG structure on the mutual coupling of a printed dipole array. *IEEE Antennas and Wireless Propagation Letters*, 4(1), 274–276. <https://doi.org/10.1109/LAWP.2005.854004>
- Abidin, Z. Z., Shah, S. M., & Ma, Y. (2018). *Miniature EBG two U-shaped slot PIFA MIMO antennas for WLAN applications*. Antenna fundamentals for legacy mobile applications and beyond (pp. 159–172). Cham: Springer International Publishing. https://doi.org/10.1007/978-3-319-63967-3_8
- Ahmed, H. S., & Elwi, T. A. (2019). On the design of a reject band filter for antennas mutual coupling reduction. *International Journal of RF and Microwave Computer-Aided Engineering*, 29(8), 1–11. <https://doi.org/10.1002/mmmc.21797>
- Al-Fayyadh, H. Q., Abdulhameed, A. A., Abdulah, A. S., & Aisabbagh, H. M. (2017). Flexible (2 × 1) MIMO antenna with electromagnetic band gap unit cell for WiMAX applications. *Turkish Journal of Electrical Engineering and Computer Sciences*, 25(4), 3061–3072. <https://doi.org/10.3906/elk-1603-94>
- Al-Fayyadh, H. Q., Alsabbagh, H. M., & Al-Rizzo, H. (2017). Flexible Compact MIMO T-Shape Antenna With Bridge Square Split Ring Resonator. *Journal of Modeling and Simulation of Antennas and Propagation*, 1–7. Retrieved from <https://www.unitedscholars.net/journal-of-modeling-and-simulation-of-antennas-and-electromagnetic-propagation.html>
- Alam, M. S., Misran, N., Yatim, B., & Islam, M. T. (2013). Development of electromagnetic band gap structures in the perspective of microstrip antenna design. *International Journal of Antennas and Propagation*, 2013, 1–22. <https://doi.org/10.1155/2013/507158>
- Aliakbari, H., & Lau, B. K. (2020). Low-Profile two-port MIMO terminal antenna for low LTE bands with wideband multimodal excitation. *IEEE Open Journal of Antennas and Propagation*, 1, 368–378. <https://doi.org/10.1109/ojap.2020.3010916>
- Alibakhshikenari, M., Khalily, M., Virdee, B. S., See, C. H., Abd-Alhameed, R. A., & Limiti, E. (2019a). Mutual-coupling isolation using embedded metamaterial EM bandgap decoupling slab for densely packed array antennas. *IEEE Access*, 7, 51827–51840. <https://doi.org/10.1109/ACCESS.2019.2909950>
- Alibakhshikenari, M., Khalily, M., Virdee, B. S., See, C. H., Abd-Alhameed, R. A., & Limiti, E. (2019b). Mutual coupling suppression between two closely placed microstrip patches using EM-bandgap metamaterial fractal loading. *IEEE Access*, 7(c), 23606–23614. <https://doi.org/10.1109/ACCESS.2019.2899326>
- Alibakhshikenari, M., Salvucci, A., Polli, G., Virdee, B. S., See, C. H., Abd-Alhameed, R., et al. (2018). *Mutual coupling reduction using metamaterial supersubstrate for high performance & densely packed planar phased arrays*. Paper presented at Micon 2018—22nd International Microwave and Radar Conference, (May) (pp. 675–678). <https://doi.org/10.23919/MIKON.2018.8405323>
- Alibakhshikenari, M., Virdee, B. S., See, C. H., & Abd-alhameed, R. (2018). Study on isolation improvement between closely packed patch antenna arrays based on fractal metamaterial electromagnetic bandgap structures study on isolation improvement between closely-packed patch antenna arrays based on fractal metamaterial electromag. *IET Microwaves, Antennas & Propagation*, 12, 2241–2247. <https://doi.org/10.1049/iet-map.2018.5103>
- Alù, A., & Engheta, N. (2005). Achieving transparency with plasmonic and metamaterial coatings. *Physical Review E: Statistical, Nonlinear and Soft Matter Physics*, 72(1), 016623. <https://doi.org/10.1103/PhysRevE.72.016623>
- Asadpor, L., & Rezvani, M. (2018). Multiband microstrip MIMO antenna with CSRR loaded for GSM and LTE applications. *Microwave and Optical Technology Letters*, 60(12), 3076–3080. <https://doi.org/10.1002/mop.31420>
- Assimonis, S. D., Yioultis, T. V., & Antonopoulos, C. S. (2012). Design and optimization of uniplanar EBG structures for coupling reduction. *IEEE Transactions on Antennas and Propagation*, 60(10), 4944–4949. <https://doi.org/10.1109/TAP.2012.2210178>
- Aydin, K., Bulu, I., Guven, K., Kafesaki, M., Soukoulis, C. M., & Ozbay, E. (2005). Investigation of magnetic resonances for different splitting resonator parameters and designs. *New Journal of Physics*, 7, 168. <https://doi.org/10.1088/1367-2630/7/1/168>
- Aydin, K., & Ozbay, E. (2006). Identifying magnetic response of split-ring resonators at microwave frequencies. *Opto-Electronics Review*, 14(3), 193–199. <https://doi.org/10.2478/s11772-006-0025-x>
- Aydin, K., & Ozbay, E. (2007). Capacitor-loaded split ring resonators as tunable metamaterial components. *Journal of Applied Physics*, 101(2), 1–5. <https://doi.org/10.1063/1.2427110>
- Baena, J. D., Bonache, J., Martín, F., Sillero, R. M., Falcone, F., Lopetegi, T., et al. (2005). Equivalent-circuit models for split-ring resonators and complementary split-ring resonators coupled to planar transmission lines. *IEEE Transactions on Microwave Theory and Techniques*, 53(4 II), 1451–1460. <https://doi.org/10.1109/TMTT.2005.845211>
- Bait-Suwailam, M. M., Boybay, M. S., & Ramahi, O. M. (2010). Electromagnetic coupling reduction in high-profile monopole antennas using single-negative magnetic metamaterials for MIMO applications. *IEEE Transactions on Antennas and Propagation*, 58(9), 2894–2902. <https://doi.org/10.1109/TAP.2010.2052560>

- Bait-Suwailam, M. M., Siddiqui, O. F., & Ramahi, O. M. (2010). Mutual coupling reduction between microstrip patch antennas using slotted-complementary split-ring resonators. *IEEE Antennas and Wireless Propagation Letters*, 9, 876–878. <https://doi.org/10.1109/LAWP.2010.2074175>
- Bernety, H. M., & Yakovlev, A. B. (2015). Reduction of mutual coupling between neighboring strip dipole antennas using confocal elliptical metasurface cloaks. *IEEE Transactions on Antennas and Propagation*, 63(4), 1554–1563. <https://doi.org/10.1109/TAP.2015.2398121>
- Bilal, M., Saleem, R., Abbasi, H. H., Shafique, M. F., & Brown, A. K. (2017). An FSS-based nonplanar quad-element UWB-MIMO antenna system. *IEEE Antennas and Wireless Propagation Letters*, 16(c), 987–990. <https://doi.org/10.1109/LAWP.2016.2615884>
- Bilal, M., Saleem, R., Shafique, M. F., & Khan, H. A. (2014). MIMO application UWB antenna doublet incorporating a sinusoidal decoupling structure. *Microwave and Optical Technology Letters*, 56(7), 1547–1553. <https://doi.org/10.1002/mop.28387>
- Bisht, M. S., Vinubhai, V. P., & Srivastava, K. V. (2020). Analysis and realization of a wideband mantle cloak with improved cloaking performance. *Journal of Electromagnetic Waves and Applications*, 34(10), 1386–1399. <https://doi.org/10.1080/09205071.2020.1726213>
- Chen, H. Y., Li, M. Q., Deng, Y. J., Weng, X. L., Xie, J. L., & Deng, L. J. (2018). Design and implementation of electromagnetic soft surfaces for decoupling in between two microstrip patch antennas. *Journal of Electromagnetic Waves and Applications*, 32(10), 1287–1297. <https://doi.org/10.1080/09205071.2018.1433075>
- Chouhan, S., Panda, D. K., Gupta, M., & Singhal, S. (2018). Multiport MIMO antennas with mutual coupling reduction techniques for modern wireless transceive operations: A review. *International Journal of RF and Microwave Computer-Aided Engineering*, 28(2), e21189. <https://doi.org/10.1002/mmce.21189>
- Cui, S., Gong, S. X., Liu, Y., Jiang, W., & Guan, Y. (2011). Compact and low coupled monopole antennas for MIMO system applications. *Journal of Electromagnetic Waves and Applications*, 25(5–6), 703–712. <https://doi.org/10.1163/156939311794827221>
- Dabas, T., Gangwar, D., Kanaujia, B. K., & Gautam, A. K. (2018). Mutual coupling reduction between elements of UWB MIMO antenna using small size uniplanar EBG exhibiting multiple stop bands. *AEU: International Journal of Electronics and Communications*, 93, 32–38. <https://doi.org/10.1016/j.aeue.2018.05.033>
- Dadgarpour, A., Zarghooni, B., Virdee, B. S., Denidni, T. A., & Kishk, A. A. (2017). Mutual coupling reduction in dielectric resonator antennas using metasurface shield for 60-GHz MIMO systems. *IEEE Antennas and Wireless Propagation Letters*, 16(c), 477–480. <https://doi.org/10.1109/LAWP.2016.2585127>
- Duan, J., Xu, K., Li, X., Chen, S., Zhao, P., & Wang, G. (2019). Dual-band and enhanced-isolation MIMO antenna with L-shaped meta-rim extended ground stubs for 5G mobile handsets. *International Journal of RF and Microwave Computer-Aided Engineering*, 29(8), 1–8. <https://doi.org/10.1002/mmce.21776>
- Ebadi, S., & Semnani, A. (2014). Mutual coupling reduction in waveguide-slot-array antennas using electromagnetic bandgap (EBG) structures. *IEEE Antennas and Propagation Magazine*, 56(3), 68–79. <https://doi.org/10.1109/MAP.2014.6867683>
- Ekmekçi, E., & Turhan-Sayan, G. (2007). Investigation of effective permittivity and permeability for a novel V-shaped metamaterial using simulated S-parameters. Paper presented at 5th International Conference on Electrical and Electronics Engineering (pp. 251–254).
- Ekrami, H., & Jam, S. (2018). A compact triple-band dual-element MIMO antenna with high port-to-port isolation for wireless applications. *AEU: International Journal of Electronics and Communications*, 96, 219–227. <https://doi.org/10.1016/j.aeue.2018.09.044>
- Exposito-Dominguez, G., Fernandez-Gonzalez, J.-M., Padilla, P., & Sierra-Castaner, M. (2012). Mutual coupling reduction using EBG in steering antennas. *IEEE Antennas and Wireless Propagation Letters*, 11, 1265–1268. <https://doi.org/10.1109/LAWP.2012.2226013>
- Farahani, H. S., Veysi, M., Kamyab, M., & Tadjalli, A. (2010). Mutual coupling reduction in patch antenna arrays using a UC-EBG superstrate. *IEEE Antennas and Wireless Propagation Letters*, 9, 57–59. <https://doi.org/10.1109/LAWP.2010.2042565>
- Gangwar, D., Das, S., & Yadava, R. L. (2014). Reduction of mutual coupling in metamaterial based microstrip antennas: The progress in last decade. *Wireless Personal Communications*, 77(4), 2747–2770. <https://doi.org/10.1007/s11277-014-1666-6>
- Garg, P., & Jain, P. (2020). Isolation improvement of MIMO antenna using a novel flower shaped metamaterial absorber at 5.5 GHz WiMAX band. *IEEE Transactions on Circuits and Systems II: Express Briefs*, 67(4), 675–679. <https://doi.org/10.1109/TCSII.2019.2925148>
- Gong, Q., Jiao, Y. C., & Gong, S. X. (2011). Compact MIMO antennas using a ring hybrid for WLAN applications. *Journal of Electromagnetic Waves and Applications*, 25(2), 431–441. <https://doi.org/10.1163/156939311794362939>
- Guo, J., Liu, F., Zhao, L., Yin, Y., Huang, G.-L., & Li, Y. (2019). Meta-surface antenna array decoupling designs for two linear polarized antennas coupled in H-plane and E-plane. *IEEE Access*, 7, 100442–100452. <https://doi.org/10.1109/access.2019.2930687>
- Han, C. Z., Xiao, L., Chen, Z., & Yuan, T. (2020). Co-located self-neutralized handset antenna pairs with complementary radiation patterns for 5G MIMO applications. *IEEE Access*, 8, 73151–73163. <https://doi.org/10.1109/ACCESS.2020.2988072>
- Hsu, C. C., Lin, K. H., & Su, H. L. (2011). Implementation of broadband isolator using metamaterial-inspired resonators and a T-shaped branch for MIMO antennas. *IEEE Transactions on Antennas and Propagation*, 59(10), 3936–3939. <https://doi.org/10.1109/TAP.2011.2163741>
- Huang, H. (2020). A decoupling method for antennas with different frequencies in 5G massive MIMO application. *IEEE Access*, 8, 140273–140278. <https://doi.org/10.1109/ACCESS.2020.3012665>
- Iqbal, A., Basir, A., Smida, A., Mallat, N. K., Elfergani, I., Rodriguez, J., & Kim, S. (2019). Electromagnetic bandgap backed millimeter-wave MIMO antenna for wearable applications. *IEEE Access*, 7, 111135–111144. <https://doi.org/10.1109/ACCESS.2019.2933913>
- Iqbal, A., Saraereh, O. A., Bouazizi, A., & Basir, A. (2018). Metamaterial-based highly isolated MIMO antenna for portable wireless applications. *Electronics*, 7(10), 3–10. <https://doi.org/10.3390/electronics7100267>
- Irene, G., & Rajesh, A. (2018a). A dual-polarized UWB-MIMO antenna with IEEE 802.11ac band-notched characteristics using split-ring resonator. *Journal of Computational Electronics*, 17(3), 1090–1098. <https://doi.org/10.1007/s10825-018-1213-x>
- Irene, G., & Rajesh, A. (2018b). Review on the design of the isolation techniques for UWB-MIMO antennas. *Advanced Electromagnetics*, 7(4), 46–70. <https://doi.org/10.7716/AEM.V7I4.743>
- Islam, M. T., & Alam, M. S. (2013). Compact EBG structure for alleviating mutual coupling between patch antenna array elements. *Progress in Electromagnetics Research*, 137, 425–438. <https://doi.org/10.2528/PIER12121205>
- Jafarholi, A., & Choi, J. H. (2019). Mutual coupling reduction in an array of patch antennas using CLL metamaterial superstrate for MIMO applications. *IEEE Transactions on Antennas and Propagation*, 67(1), 179–189. <https://doi.org/10.1109/TAP.2018.2874747>
- Jehangir, S. S., & Sharawi, M. S. (2017). A single layer semi-ring slot Yagi-like MIMO antenna system with high front-to-back ratio. *IEEE Transactions on Antennas and Propagation*, 65(2), 937–942. <https://doi.org/10.1109/TAP.2016.2633938>
- Jiang, T., Jiao, T., & Li, Y. (2018). A low mutual coupling MIMO antenna using periodic multi-layered electromagnetic band gap structures. *ACES Journal*, 33(3), 305–311.
- Jiang, W., Liu, B., Cui, Y., & Hu, W. (2019). High-isolation eight-element MIMO array for 5G smartphone applications. *IEEE Access*, 7, 34104–34112. <https://doi.org/10.1109/ACCESS.2019.2904647>

- Jiang, Z. H., Sieber, P. E., Kang, L., & Werner, D. H. (2015). Restoring intrinsic properties of electromagnetic radiators using ultralight-weight integrated metasurface cloaks. *Advanced Functional Materials*, 25(29), 4708–4716. <https://doi.org/10.1002/adfm.201501261>
- Jin, Y., Ko, M., Yeonjeong, O., & Choi, J. (2019). A planar UWB MIMO antenna with gain enhancement and isolation improvement for the 5G mobile platform. *Microwave and Optical Technology Letters*, 61(4), 990–998. <https://doi.org/10.1002/mop.31685>
- John, S. (1987). Strong localization of photons in certain disordered dielectric superlattices. *Physical Review Letters*, 58(23), 2486–2489. <https://doi.org/10.1103/PhysRevLett.58.2486>
- Kapoor, M. (2013). *CHAPTER -3 electromagnetic BandGap structures*. Ph.D. Dissertation. Agra, India: Dayalbagh Educational Institute.
- Katsarakis, N., Koschny, T., Kafesaki, M., Economou, E. N., & Soukoulis, C. M. (2004). Electric coupling to the magnetic resonance of split ring resonators. *Applied Physics Letters*, 84(15), 2943–2945. <https://doi.org/10.1063/1.1695439>
- Kayabasi, A., Toktas, A., Yigit, E., & Sabanci, K. (2018). Triangular quad-port multi-polarized UWB MIMO antenna with enhanced isolation using neutralization ring. *AEU: International Journal of Electronics and Communications*, 85, 47–53. <https://doi.org/10.1016/j.aeue.2017.12.027>
- Khan, M. S., Capobianco, A. D., Najam, A. I., Shoaib, I., Autizi, E., & Shafique, M. F. (2014). Compact ultra-wideband diversity antenna with a floating parasitic digitated decoupling structure. *IET Microwaves, Antennas & Propagation*, 8(10), 747–753. <https://doi.org/10.1049/iet-map.2013.0672>
- Khan, M. U., & Sharawi, M. S. (2014). *Isolation improvement using an MTM inspired structure with a patch based MIMO antenna system*. Paper presented at 8th European conference on antennas and propagation, EuCAP 2014, (EuCAP) (pp. 2718–2722). <https://doi.org/10.1109/EuCAP.2014.6902386>
- Kim, S.-H., Nguyen, T. T., & Jang, J.-H. (2011). Reflection characteristics OF 1-D EBG ground plane and its application to a planar dipole antenna. *Progress in Electromagnetics Research*, 120, 51–66. <https://doi.org/10.2528/PIER11062909>
- Krishna, K. V., Naidu, P. R. T., Shaik, L. A., Saha, C., & Siddiqui, J. Y. (2016). *Printed ultrawide band- narrow band antenna pair with enhanced isolation for MIMO applications*. Paper presented at 2015 IEEE applied electromagnetics conference, AEMC 2015 (February 2017). <https://doi.org/10.1109/AEMC.2015.7509205>
- Kumar, A., Ansari, A. Q., Kanaujia, B. K., & Kishor, J. (2018). High isolation compact four-port MIMO antenna loaded with CSRR for multiband applications. *Frequenz*, 72(9–10), 415–427. <https://doi.org/10.1515/freq-2017-0276>
- Kumar, A., Ansari, A. Q., Kanaujia, B. K., & Kishor, J. (2019). A novel ITI-shaped isolation structure placed between two-port CPW-fed dual-band MIMO antenna for high isolation. *AEU: International Journal of Electronics and Communications*, 104, 35–43. <https://doi.org/10.1016/j.aeue.2019.03.009>
- Kumar, A., Ansari, A. Q., Kanaujia, B. K., Kishor, J., & Kandpal, P. (2018). *Design of CPW-Fed triple-band two-port MIMO antenna with U-Shaped slot isolation structure for high isolation*. Paper presented at IEEE MTT-S International Microwave and RF Conference, IMaRC 2018 (pp. 1–4). Institute of Electrical and Electronics Engineers Inc. <https://doi.org/10.1109/IMaRC.2018.8877330>
- Kumar, A., Ansari, A. Q., Kanaujia, B. K., Kishor, J., & Kumar, S. (2020). An ultra-compact two-port UWB-MIMO antenna with dual band-notched characteristics. *AEU: International Journal of Electronics and Communications*, 114, 152997. <https://doi.org/10.1016/j.aeue.2019.152997>
- Kumar, A., Ansari, A. Q., Kanaujia, B. K., Kishor, J., & Tewari, N. (2018). Design of triple-band MIMO antenna with one band-notched characteristic. *Progress in Electromagnetics Research C*, 86, 41–53. <https://doi.org/10.2528/PIERC18051902>
- Kumar, J. (2016). Compact MIMO antenna. *Microwave and Optical Technology Letters*, 58(6), 1294–1298. <https://doi.org/10.1002/mop.29843>
- Kumar, N., & Kommuri, U. K. (2019). MIMO antenna H-plane isolation enhancement using UC-EBG structure and metal line strip for WLAN applications. *Radioengineering*, 27(2), 399–406. <https://doi.org/10.13164/RE.2019.0399>
- Kumar, S., Kumar, R., Kumar Vishwakarma, R., & Srivastava, K. (2018). An improved compact MIMO antenna for wireless applications with band-notched characteristics. *AEU: International Journal of Electronics and Communications*, 90, 20–29. <https://doi.org/10.1016/j.aeue.2018.04.008>
- Lee, J. Y., Kim, S. H., & Jang, J. H. (2015). Reduction of mutual coupling in planar multiple antenna by using 1-D EBG and SRR structures. *IEEE Transactions on Antennas and Propagation*, 63(9), 4194–4198. <https://doi.org/10.1109/TAP.2015.2447052>
- Lee, Y., & Sun, J. (2008). Bow-tie antenna using high-impedance ground plane. *Microwave and Optical Technology Letters*, 50(11), 2928–2931. <https://doi.org/10.1002/mop.23807>
- Li, J., & Pendry, J. B. (2008). Hiding under the carpet: A new strategy for cloaking. *Physical Review Letters*, 101(20), 1–4. <https://doi.org/10.1103/PhysRevLett.101.203901>
- Li, M., Chen, X., Zhang, A., Fan, W., & Kishk, A. A. (2020). Split ring resonator loaded baffles for decoupling of dual-polarized base station array. *IEEE Antennas and Wireless Propagation Letters*, 1225, 1828–1832. <https://doi.org/10.1109/lawp.2020.3020855>
- Li, Q., Ieee, M., Feresidis, A. P., Ieee, M., Mavridou, M., & Hall, P. S. (2014). Miniaturized double-layer EBG structures for broadband mutual coupling reduction between UWB monopoles. *IEEE Transactions on Antennas and Propagation*, 63, 18–21. <https://doi.org/10.1109/TAP.2014.2387871>
- Lin, X. Q., Li, H., He, S., & Fan, Y. (2012). A decoupling technique for increasing the port isolation between two closely packed antennas. *IEEE Antennas and Propagation Society, AP-S International Symposium (Digest)*, 56(12), 3650–3658. <https://doi.org/10.1109/APS.2012.6349240>
- Ling, X., & Li, R. (2011). A novel dual-band MIMO antenna array with low mutual coupling for portable wireless devices. *IEEE Antennas and Wireless Propagation Letters*, 10, 1039–1042. <https://doi.org/10.1109/LAWP.2011.2169035>
- Liu, F., Guo, J., Zhao, L., Huang, G. L., Li, Y., & Yin, Y. (2020). Dual-band metasurface-based decoupling method for two closely packed dual-band Antennas. *IEEE Transactions on Antennas and Propagation*, 68(1), 552–557. <https://doi.org/10.1109/TAP.2019.2940316>
- Liu, L., Cheung, S. W., & Yuk, T. I. (2014). Compact multiple-input-multiple-output antenna using quasi-self-complementary antenna structures for ultrawideband applications. *IET Microwaves, Antennas & Propagation*, 8(13), 1021–1029. <https://doi.org/10.1049/iet-map.2013.0503>
- Liu, R., An, X., Zheng, H., Wang, M., Gao, Z., & Li, E. (2020). Neutralization line decoupling tri-band multiple-input multiple-output antenna design. *IEEE Access*, 8, 27018–27026. <https://doi.org/10.1109/ACCESS.2020.2971038>
- Liu, X. L., Wang, Z. D., Yin, Y. Z., Ren, J., & Wu, J. J. (2014). A compact ultrawideband MIMO antenna using QSCA for high isolation. *IEEE Antennas and Wireless Propagation Letters*, 13, 1497–1500. <https://doi.org/10.1109/LAWP.2014.2340395>
- Lu, Y. F., & Lin, Y. C. (2013). Electromagnetic band-gap based corrugated structures for reducing mutual coupling of compact 60 GHz cavity-backed antenna arrays in low temperature co-fired ceramics. *IET Microwaves, Antennas & Propagation*, 7(9), 754–759. <https://doi.org/10.1049/iet-map.2012.0674>
- Luo, S., Li, Y., Xia, Y., & Zhang, L. (2019). A low mutual coupling antenna array with gain enhancement using metamaterial loading and neutralization line structure. *Applied Computational Electromagnetics Society Journal*, 34(3), 411–418.

- Malekpour, N., & Honarvar, M. A. (2016). Design of high-isolation compact MIMO antenna for UWB application. *Progress in Electromagnetics Research C*, 62, 119–129. <https://doi.org/10.2528/PIERC15120902>
- Malik, J., Patnaik, A., & Kartikeyan, M. V. (2015). Novel printed MIMO antenna with pattern and polarization diversity. *IEEE Antennas and Wireless Propagation Letters*, 14(c), 739–742. <https://doi.org/10.1109/LAWP.2014.2377784>
- Malviya, L., Panigrahi, R. K., & Kartikeyan, M. V. (2017). MIMO antennas with diversity and mutual coupling reduction techniques: A review. *International Journal of Microwave and Wireless Technologies*, 9(8), 1763–1780. <https://doi.org/10.1017/S1759078717000538>
- Manimegalai, D. H., Subasree, M. R., Susithra, S., Keerthika, S. S., & Manimegalai, B. (2014). *Mutual coupling reduction in MIMO antenna system using EBG structures*. Paper presented at 2012 international conference on signal processing and communications (SPCOM). IEEE. <https://doi.org/10.1109/SPCOM.2012.6290217>
- Mark, R., Singh, H. V., Mandal, K., & Das, S. (2020). Mutual coupling reduction using near-zero ϵ and μ metamaterial-based superstrate for an MIMO application. *IET Microwaves, Antennas & Propagation*, 14(6), 479–484. <https://doi.org/10.1049/iet-map.2019.0382>
- Mavridou, M., Feresidis, A. P., & Gardner, P. (2016). Tunable double-layer EBG structures and application to antenna isolation. *IEEE Transactions on Antennas and Propagation*, 64(1), 70–79. <https://doi.org/10.1109/TAP.2015.2496619>
- Mazaheri, M. H., & Jafarholi, A. (2018). A broadband array antenna using epsilon-near-zero metamaterials for MIMO applications. *International Journal of RF and Microwave Computer-Aided Engineering*, 28(7), 1–10. <https://doi.org/10.1002/mmce.21475>
- Mohamed, I., Abdalla, M., & Mitkees, A. E. A. (2019). Perfect isolation performance among two-element MIMO antennas. *AEUE: International Journal of Electronics and Communications*, 107, 21–31. <https://doi.org/10.1016/j.aeue.2019.05.014>
- Mohamadzade, B., & Afsahi, M. (2017). Mutual coupling reduction and gain enhancement in patch array antenna using a planar compact electromagnetic bandgap structure. *IET Microwaves, Antennas & Propagation*, 11(12), 1719–1725. <https://doi.org/10.1049/iet-map.2017.0080>
- Moharram, M. A., & Kishk, A. A. (2013). General decoupling network design between two coupled antennas for MIMO applications. *Progress in Electromagnetics Research Letters*, 37, 133–142. <https://doi.org/10.2528/PIERL12121908>
- Mondal, P., Dhara, D., & Harish, A. R. (2018). *A wideband slotted D-shaped monopole MIMO antenna with triple branch neutralization line*. Paper presented at 2018 IEEE Indian conference on antennas and propagation, InCAP 2018, (July) (pp. 1–4). IEEE. <https://doi.org/10.1109/INCAP.2018.8770733>
- Moreno, G., Mehrpour Bernety, H., & Yakovlev, A. B. (2016). Reduction of mutual coupling between strip dipole antennas at terahertz frequencies with an elliptically shaped graphene monolayer. *IEEE Antennas and Wireless Propagation Letters*, 15, 1533–1536. <https://doi.org/10.1109/LAWP.2015.2505333>
- Mu'ath, J. Al-Hasan, Denidni, T. A., & Sebak, A. R. (2014). Millimeter-wave compact EBG structure for mutual coupling reduction applications. *IEEE Transactions on Antennas and Propagation*, 63, 823–828. <https://doi.org/10.1109/TAP.2014.2381229>
- Nadeem, I., & Choi, D.-Y. (2019). Study on mutual coupling reduction technique for MIMO antennas. *IEEE Access*, 7, 563–586. <https://doi.org/10.1109/ACCESS.2018.2885558>
- Najafy, V., & Bemani, M. (2020). Mutual-coupling reduction in triple-band MIMO antennas for WLAN using CSRRs. *International Journal of Microwave and Wireless Technologies*, 12(8), 762–768. <https://doi.org/10.1017/S1759078720000215>
- Naqvi, A., Saeed Khan, M., & Braaten, B. D. (2016). A frequency reconfigurable cylindrically shaped surface with cloaking-like properties. *Microwave and Optical Technology Letters*, 58(6), 1323–1329. <https://doi.org/10.1002/mop.29793>
- Ntaikos, D. K., & Yioultis, T. V. (2013). Compact split-ring resonator-loaded multiple-input-multiple-output antenna with electrically small elements and reduced mutual coupling. *IET Microwaves, Antennas & Propagation*, 7(6), 421–429. <https://doi.org/10.1049/iet-map.2012.0688>
- Ou, Y., Cai, X., & Qian, K. (2017). Two-element compact antennas decoupled with a simple neutralization line. *Progress in Electromagnetics Research Letters*, 65, 63–68. <https://doi.org/10.2528/PIERL16111801>
- Öznazi, V., & Ertürk, V. B. (2008). A comparative investigation of SRR- and CSRR-based band-reject filters: Simulations, experiments, and discussions. *Microwave and Optical Technology Letters*, 50(2), 519–523. <https://doi.org/10.1002/mop.23119>
- Padilla, W. J., Basov, D. N., & Smith, D. R. (2006). Negative refractive index metamaterials. *Materials Today*, 9(7–8), 28–35. [https://doi.org/10.1016/S1369-7021\(06\)71573-5](https://doi.org/10.1016/S1369-7021(06)71573-5)
- Park, C. H., & Son, H. W. (2016). Mutual coupling reduction between closely spaced microstrip antennas by means of H-shaped conducting wall. *Electronics Letters*, 52(13), 1093–1094. <https://doi.org/10.1049/el.2016.1339>
- Payandehjoo, K., & Abhari, R. (2009). Employing EBG structures in multiantenna systems for improving isolation and diversity gain. *IEEE Antennas and Wireless Propagation Letters*, 8, 1162–1165. <https://doi.org/10.1109/LAWP.2009.2034877>
- Payandehjoo, K., & Abhari, R. (2014). Isolation enhancement between tightly spaced compact unidirectional patch-antennas on multilayer EBG surfaces. *International Journal of RF and Microwave Computer-Aided Engineering*, 25(1), 30–38. <https://doi.org/10.1002/mmce.20820>
- Pendry, J. B., Holden, A. J., Robbins, D. J., & Stewart, W. J. (1999). Magnetism from conductors and enhanced nonlinear phenomena. *IEEE Transactions on Microwave Theory and Techniques*, 47(11), 2075–2084. <https://doi.org/10.1109/22.798002>
- Pendry, J. B., Schurig, D., & Smith, D. R. (2006). Controlling electromagnetic fields. *Science*, 312(5781), 1780–1782. <https://doi.org/10.1126/science.1125907>
- Piao, H., Jin, Y., Xu, Y., & Qu, L. (2020). MIMO ground-radiation antennas using a novel closed-decoupling-loop for 5G applications. *IEEE Access*, 8, 142714–142724. <https://doi.org/10.1109/ACCESS.2020.3014243>
- Qamar, Z., Naeem, U., Khan, S. A., Chongcheawchamnan, M., & Shafique, M. F. (2016). Mutual coupling reduction for high-performance densely packed patch antenna arrays on finite substrate. *IEEE Transactions on Antennas and Propagation*, 64(5), 1653–1660. <https://doi.org/10.1109/TAP.2016.2535540>
- Qamar, Z., Riaz, L., Chongcheawchamnan, M., Khan, S. A., & Shafique, M. F. (2014). Slot combined complementary split ring resonators for mutual coupling suppression in microstrip phased arrays. *IET Microwaves, Antennas & Propagation*, 8(15), 1261–1267. <https://doi.org/10.1049/iet-map.2013.0541>
- Radhi, A. H., Nilavalan, R., Wang, Y., Al-Raweshidy, H. S., Eltokhy, A. A., & Ab Aziz, N. (2018). Mutual coupling reduction with a wideband planar decoupling structure for UWB-MIMO antennas. *International Journal of Microwave and Wireless Technologies*, 10(10), 1143–1154. <https://doi.org/10.1017/S1759078718001010>
- Radhi, A. H., Nilavalan, R., Wang, Y., Eltokhy, A. A., & Aziz, N. A. (2019). Mutual coupling reduction with a novel fractal electromagnetic band gap structure. *IET Microwaves, Antennas & Propagation*, 13(2), 134–141.
- Rajo-Iglesias, E., Quevedo-Teruel, Ó., & Inclán-Sánchez, L. (2008). Mutual coupling reduction in patch antenna arrays by using a planar EBG structure and a multilayer dielectric substrate. *IEEE Transactions on Antennas and Propagation*, 56(6), 1648–1655. <https://doi.org/10.1109/TAP.2008.923306>

- Ramachandran, A., Mathew, S., Rajan, V., & Kesavath, V. (2017). A compact triband quad-element MIMO antenna using SRR ring for high isolation. *IEEE Antennas and Wireless Propagation Letters*, 16, 1409–1412. <https://doi.org/10.1109/LAWP.2016.2640305>
- Ramachandran, A., Valiyaveetil Pushpakaran, S., Pezhohil, M., & Kesavath, V. (2016). A four-port MIMO antenna using concentric square-ring patches loaded with CSRR for high isolation. *IEEE Antennas and Wireless Propagation Letters*, 15(c), 1196–1199. <https://doi.org/10.1109/LAWP.2015.2499322>
- Saleh, A. M., Sayidmarie, K. H., Abd-Alhameed, R. A., Jones, S., Noras, J. M., & Excell, P. S. (2017). *Compact tri-band MIMO antenna with high port isolation for WLAN and WiMAX applications*. Paper presented at 2016 loughborough antennas and propagation conference, LAPC 2016 (pp. 5–8). <https://doi.org/10.1109/LAPC.2016.7807546>
- Sauviac, B., Simovski, C. R., & Tretyakov, S. A. (2004). Double split-ring resonators: Analytical modeling and numerical simulations. *Electromagnetics*, 24(5), 317–338. <https://doi.org/10.1080/02726340490457890>
- Selvaraju, R., Jamaluddin, M. H., Kamarudin, M. R., Nasir, J., & Dahri, M. H. (2018a). Complementary split ring resonator for isolation enhancement in 5G communication antenna array. *Progress in Electromagnetics Research C*, 83, 217–228. <https://doi.org/10.2528/PIERC18011019>
- Selvaraju, R., Jamaluddin, M. H., Kamarudin, M. R., Nasir, J., & Dahri, M. H. (2018b). Mutual coupling reduction and pattern error correction in a 5G beamforming linear array using CSRR. *IEEE Access*, 6, 65922–65934. <https://doi.org/10.1109/ACCESS.2018.2873062>
- Shabbir, T., Saleem, R., Al-Bawri, S. S., Shafique, M. F., & Islam, M. T. (2020). Eight-port metamaterial loaded UWB-MIMO antenna system for 3D system-in-package applications. *IEEE Access*, 8, 106982–106992. <https://doi.org/10.1109/ACCESS.2020.3000134>
- Shafique, M. F., Qamar, Z., Riaz, L., Saleem, R., & Khan, S. A. (2015). Coupling suppression in densely packed microstrip arrays using metamaterial structure. *Microwave and Optical Technology Letters*, 57(3), 759–763. <https://doi.org/10.1002/mop.28943>
- Sharawi, M. S. (2017). Current misuses and future prospects for printed multiple-input, multiple-output antenna systems [wireless corner]. *IEEE Antennas and Propagation Magazine*, 59(2), 162–170. <https://doi.org/10.1109/MAP.2017.2658346>
- Sharma, K., & Pandey, G. P. (2020). Two port compact MIMO antenna for ISM band applications. *Progress in Electromagnetics Research C*, 100, 173–185. <https://doi.org/10.2528/PIERC20011504>
- Shen, X., Liu, Y., Zhao, L., Huang, G. L., Shi, X., & Huang, Q. (2019). A miniaturized microstrip antenna array at 5G millimeter-wave band. *IEEE Antennas and Wireless Propagation Letters*, 18(8), 1671–1675. <https://doi.org/10.1109/LAWP.2019.2927460>
- Shumpert, J. D., Ellis, T. J., Rebeiz, G. M., & Katehi, L. P. (1997). *Microwave and millimeter-wave propagation in photonic band-gap structures*. University of Michigan. Radiation Laboratory. Retrieved from <http://hdl.handle.net/2027.42/21090>
- Singh, H. S., Meruva, B., Pandey, G. K., Bharti, P. K., & Meshram, M. K. (2013). *Progress In Electromagnetics Research B*, 53, 205–221. <https://doi.org/10.2528/PIERB13020115>
- Sipal, D., Abegaonkar, M. P., & Koul, S. K. (2018). *Compact planar four element dual band-notched UWB MIMO antenna for personal area network applications*. IET Conference Publications CP741 (Vol. 2018, pp. 1–5). <https://doi.org/10.1049/cp.2018.0458>
- Sipal, D., Abegaonkar, M. P., & Koul, S. K. (2019). Highly isolated compact planar dual-band Antenna with polarization/pattern diversity characteristics for MIMO terminals. *IEEE Antennas and Wireless Propagation Letters*, 18(4), 762–766. <https://doi.org/10.1109/LAWP.2019.2902247>
- Smith, D. R., Pendry, J. B., & Wiltshire, M. C. K. (2004). Metamaterials and negative refractive index. *Science*, 305(5685), 788–792. <https://doi.org/10.1126/science.1096796>
- Smith, D. R., Schultz, S., Markoš, P., & Soukoulis, C. M. (2002). Determination of effective permittivity and permeability of metamaterials from reflection and transmission coefficients. *Physical Review B: Condensed Matter and Materials Physics*, 65(19), 1–5. <https://doi.org/10.1103/PhysRevB.65.195104>
- Soliman, A. M., Elsheakh, D. M., Abdallah, E. A., & El-Hennawy, H. (2015). Design of planar inverted-F antenna over uniplanar EBG structure for laptop MIMO applications. *Microwave and Optical Technology Letters*, 57(2), 277–285. <https://doi.org/10.1002/mop.28828>
- Soukoulis, C. M. (2002). *The history and a review of the modelling and fabrication of photonic crystals* (Vol. 13). Institute of Physics Publishing. <https://doi.org/10.1088/0957-4484/13/3/335>
- Su, S.-W., & Lee, C.-T. (2011). Printed two monopole-antenna system with a decoupling neutralization line for 2.4-GHz MIMO applications. *Microwave and Optical Technology Letters*, 53(9), 2037–2043. <https://doi.org/10.1002/mop.26199>
- Sun, L., Li, Y., Zhang, Z., & Wang, H. (2020). Self-decoupled MIMO antenna pair with shared radiator for 5G smartphones. *IEEE Transactions on Antennas and Propagation*, 68(5), 3423–3432. <https://doi.org/10.1109/TAP.2019.2963664>
- Suntives, A., & Abhari, R. (2013). Miniaturization and isolation improvement of a multiple-patch antenna system using electromagnetic bandgap structures. *Microwave and Optical Technology Letters*, 55(7), 1609–1612. <https://doi.org/10.1002/mop.27621>
- Tan, X., Wang, W., Wu, Y., Liu, Y., & Kishk, A. A. (2019). Enhancing isolation in dual-band meander-line multiple antenna by employing split EBG structure. *IEEE Transactions on Antennas and Propagation*, 67(4), 2769–2774. <https://doi.org/10.1109/TAP.2019.2897489>
- Tang, M. C., Chen, Z., Wang, H., Li, M., Luo, B., Wang, J., et al. (2017). Mutual coupling reduction using meta-structures for wideband, dual-polarized, and high-density patch arrays. *IEEE Transactions on Antennas and Propagation*, 65(8), 3986–3998. <https://doi.org/10.1109/TAP.2017.2710214>
- Tang, T. C., & Lin, K. H. (2014). An ultrawideband MIMO antenna with dual band-notched function. *IEEE Antennas and Wireless Propagation Letters*, 13, 1076–1079. <https://doi.org/10.1109/LAWP.2014.2329496>
- Tang, Z., Wu, X., Zhan, J., Hu, S., Xi, Z., & Liu, Y. (2019). Compact UWB-MIMO antenna with high isolation and triple band-notched characteristics. *IEEE Access*, 7, 19856–19865. <https://doi.org/10.1109/ACCESS.2019.2897170>
- Thakur, E., Jaglan, N., & Gupta, S. D. (2020). Design of compact triple band-notched UWB MIMO antenna with TVC-EBG structure. *Journal of Electromagnetic Waves and Applications*, 34(11), 1601–1615. <https://doi.org/10.1080/09205071.2020.1775136>
- Thummaluru, S. R., & Chaudhary, R. K. (2017). Mu-negative metamaterial filter-based isolation technique for MIMO antennas. *Electronics Letters*, 53(10), 644–646. <https://doi.org/10.1049/el.2017.0809>
- Tiwari, R. N., Singh, P., & Kanaujia, B. K. (2019). A compact UWB MIMO antenna with neutralization line for WLAN/ISM/mobile applications. *International Journal of RF and Microwave Computer-Aided Engineering*, 29(11), 1–9. <https://doi.org/10.1002/mmce.21907>
- Tiwari, R. N., Singh, P., Kanaujia, B. K., & Srivastava, K. (2019). Neutralization technique based two and four port high isolation MIMO antennas for UWB communication. *AEU - International Journal of Electronics and Communications*, 110, 152828. <https://doi.org/10.1016/j.aeue.2019.152828>
- Toolabi, M., Sadeghzadeh, R. A., & Nasser-Moghadasi, M. (2016). Compact meandered-shape electromagnetic bandgap structure using in a microstrip array antenna application. *Microwave and Optical Technology Letters*, 58(9), 2084–2088. <https://doi.org/10.1002/mop.29982>
- Torabi, Y., Bahri, A., & Sharihi, A. R. (2016). A novel metamaterial MIMO antenna with improved isolation and compact size based on LSRR resonator. *IETE Journal of Research*, 62(1), 106–112. <https://doi.org/10.1080/03772063.2015.1085335>

- Veselago, V. G. (1968). The electrodynamics of substances with simultaneously negative values of ϵ and μ . *Soviet Physics: Uspekhi*, 10(4), 509–514. <https://doi.org/10.1070/PU1968v010n04ABEH003699>
- Wang, F., Duan, Z., Li, S., Wang, Z., & Gong, Y. (2018). Compact UWB MIMO antenna with metamaterial-inspired isolator. *Progress In Electromagnetics Research C*, 84, 61–74. <https://doi.org/10.2528/PIERC18030201>
- Wang, H., Liu, L., Zhang, Z., Li, Y., & Feng, Z. (2014). Ultra-compact three-port MIMO antenna with high isolation and directional radiation patterns. *IEEE Antennas and Wireless Propagation Letters*, 13, 1545–1548. <https://doi.org/10.1109/LAWP.2014.2344104>
- Wang, H., Zhang, Z., & Feng, Z. (2015). Dual-port planar MIMO antenna with ultra-high isolation and orthogonal radiation patterns. *Electronics Letters*, 51(1), 7–8. <https://doi.org/10.1049/el.2014.2998>
- Wang, J., Qu, S., Xu, Z., Ma, H., Yang, Y., & Gu, C. (2008). A controllable magnetic metamaterial: Split-ring resonator with rotated inner ring. *IEEE Transactions on Antennas and Propagation*, 56(7), 2018–2022. <https://doi.org/10.1109/TAP.2008.924728>
- Wang, S., & Du, Z. (2015). Decoupled dual-antenna system using crossed neutralization lines for LTE/WWAN smartphone applications. *IEEE Antennas and Wireless Propagation Letters*, 14, 523–526. <https://doi.org/10.1109/LAWP.2014.2371020>
- Wang, S. M., Hwang, L. T., Lee, C. J., Hsu, C. Y., & Chang, F. S. (2015). MIMO antenna design with built-in decoupling mechanism for WLAN dual-band applications. *Electronics Letters*, 51(13), 966–968. <https://doi.org/10.1049/el.2014.4352>
- Wang, Y., & Du, Z. (2014). A wideband printed dual-antenna with three neutralization lines for mobile terminals. *IEEE Transactions on Antennas and Propagation*, 62(3), 1495–1500. <https://doi.org/10.1109/TAP.2013.2295226>
- Wang, Z., Li, C., & Yin, Y. (2020). A meta-surface antenna array decoupling (MAAD) design to improve the isolation performance in a MIMO system. *IEEE Access*, 8, 61797–61805. <https://doi.org/10.1109/ACCESS.2020.2983482>
- Wong, K. L., Tsai, C. Y., & Lu, J. Y. (2017). Two asymmetrically mirrored gap-coupled loop antennas as a compact building block for eight-antenna MIMO array in the future smartphone. *IEEE Transactions on Antennas and Propagation*, 65(4), 1765–1778. <https://doi.org/10.1109/TAP.2017.2670534>
- Wu, G.-C., Wang, G.-M., Liang, J.-G., Gao, X.-J., & Zhu, L. (2015). Novel ultra-compact two-dimensional waveguide-based metasurface for electromagnetic coupling reduction of microstrip antenna array. *International Journal of RF and Microwave Computer-Aided Engineering*, 25(9), 789–794. <https://doi.org/10.1002/mmce.20917>
- Wu, W., Yuan, B., & Wu, A. (2018). A quad-element UWB-MIMO antenna with band-notch and reduced mutual coupling based on EBG structures. *International Journal of Antennas and Propagation*, 2018. <https://doi.org/https://doi.org/10.1155/2018/8490740>
- Xu, H. X., Wang, G. M., & Qi, M. Q. (2013). Hilbert-shaped magnetic waveguided metamaterials for electromagnetic coupling reduction of microstrip antenna array. *IEEE Transactions on Magnetics*, 49(4), 1526–1529. <https://doi.org/10.1109/TMAG.2012.2230272>
- Xu, K. D., Luyen, H., & Behdad, N. (2020). A decoupling and matching network design for single-and dual-band two-element antenna arrays. *IEEE Transactions on Microwave Theory and Techniques*, 68(9), 3986–3999. <https://doi.org/10.1109/TMTT.2020.2989120>
- Xu, K. D., Zhu, J., Liao, S., & Xue, Q. (2018). Wideband patch antenna using multiple parasitic patches and its array application with mutual coupling reduction. *IEEE Access*, 6, 42497–42506. <https://doi.org/10.1109/ACCESS.2018.2860594>
- Xun, J. H., Shi, L. F., Liu, W. R., Liu, G. X., & Chen, S. (2017). Compact dual-band decoupling structure for improving mutual coupling of closely placed PIFAs. *IEEE Antennas and Wireless Propagation Letters*, 16, 1985–1989. <https://doi.org/10.1109/LAWP.2017.2691716>
- Yablonovitch, E. (1987). Inhibited spontaneous emission in solid-state physics and electronics. *Physical Review Letters*, 58(20), 2059–2062. <https://doi.org/10.1103/PhysRevLett.58.2059>
- Yang, X. M., Liu, X. G., Zhou, X. Y., Cui, T. J., & Member, S. (2012). Reduction of mutual coupling between closely packed patch antennas using metamaterials. *IEEE Antennas and Wireless Propagation Letters*, 11, 389–391. <https://doi.org/10.1109/LAWP.2012.2193111>
- Yang, Y., Chu, Q., & Mao, C. (2016). Multiband MIMO antenna for GSM, DCS, and LTE indoor applications. *IEEE Antennas and Wireless Propagation Letters*, 15, 1573–1576. <https://doi.org/10.1109/LAWP.2016.2517188>
- Yin, B., Feng, X., & Gu, J. (2020). A metasurface wall for isolation enhancement: Minimizing mutual coupling between MIMO antenna elements. *IEEE Antennas and Propagation Magazine*, 62(1), 14–22. <https://doi.org/10.1109/MAP.2019.2943299>
- Yu, A., & Zhang, X. (2003). A novel method to improve the performance of microstrip antenna arrays using a dumbbell EBG structure. *IEEE Antennas and Wireless Propagation Letters*, 2, 170–172. <https://doi.org/10.1109/LAWP.2003.814773>
- Yu, K., Li, Y., & Liu, X. (2018). Mutual coupling reduction of a MIMO antenna array using 3-D novel meta-material structures. *Applied Computational Electromagnetics Society Journal*, 33(7), 758–763.
- Yu, Y., Liu, X., Gu, Z., & Yi, L. (2016). A compact printed monopole array with neutralization line for UWB applications. *Paper presented at 2016 IEEE antennas and propagation society international symposium, APSURSI 2016—proceedings* (pp. 1779–1780). IEEE. <https://doi.org/10.1109/APS.2016.7696596>
- Zaker, R. (2018). Design of a very closely-spaced antenna array with a high reduction of mutual coupling using novel parasitic L-shaped strips. *International Journal of RF and Microwave Computer-Aided Engineering*, 28(9), e21422. <https://doi.org/10.1002/mmce.21422>
- Zhai, G., Chen, Z. N., & Qing, X. (2015). Enhanced isolation of a closely spaced four-element MIMO antenna system using metamaterial mushroom. *IEEE Transactions on Antennas and Propagation*, 63(8), 3362–3370. <https://doi.org/10.1109/TAP.2015.2434403>
- Zhang, S., & Pedersen, G. F. (2016). Mutual coupling reduction for UWB MIMO antennas with a wideband neutralization line. *IEEE Antennas and Wireless Propagation Letters*, 15(c), 166–169. <https://doi.org/10.1109/LAWP.2015.2435992>
- Zheng, Q.-R., Fu, Y.-Q., & N.-C. Y. (2008). A novel compact spiral electromagnetic band-gap (EBG) structure. *IEEE Transactions on Antennas and Propagation*, 56(6), 1656–1660. <https://doi.org/10.1109/TAP.2008.923305>
- Zhu, J., & Eleftheriades, G. V. (2010). A simple approach to reducing mutual coupling in two closely-spaced electrically small antennas. *IEEE Antennas and Wireless Propagation Letters*, 9, 379–382. <https://doi.org/10.1109/APS.2010.5561228>
- Zhu, J., Feng, B., Peng, B., Deng, L., & Li, S. (2016). A dual notched band MIMO slot antenna system with Y-shaped defected ground structure for UWB applications. *Microwave and Optical Technology Letters*, 58(3), 626–630. <https://doi.org/10.1002/mop.29632>
- Zhu, J., Feng, B., Peng, B., Deng, L., & Li, S. (2017). Multiband printed mobile MIMO antenna for WWAN and LTE applications. *Microwave and Optical Technology Letters*, 59(6), 1446–1450. <https://doi.org/10.1002/mop.30567>
- Zhu, X., Yang, X., Song, Q., & Lui, B. (2017). Compact UWB-MIMO antenna with metamaterial FSS decoupling structure. *EURASIP Journal on Wireless Communications and Networking*, 2017(1), 0–5. <https://doi.org/10.1186/s13638-017-0894-3>
- Ziolkowski, R. W., & Engheta, N. (2020). Metamaterials: Two decades past and into their electromagnetics future and beyond. *IEEE Transactions on Antennas and Propagation*, 68(3), 1232–1237. <https://doi.org/10.1109/TAP.2019.2938674>